applied sciences

MDPI

Review

Aggregation-Induced Emission (AIE) Probes in Fluorescent Sensing: Progress and Applications for Pesticide Detection

Bowen Zha [1], Hui Li [2,*], Susu Ren [1], Jia-Rui Wu [1,*] and Haitao Wang [1,*]

[1] Key Laboratory of Automobile Materials, MOE, School of Materials Science and Engineering, Jilin University, Changchun 130012, China; zhabowen1999@163.com (B.Z.); renss24@mails.jlu.edu.cn (S.R.)
[2] School of Chemistry and Life Science, Advanced Institute of Materials Science, Changchun University of Technology, 2055 Yanan Street, Changchun 130012, China
* Correspondence: lihui247@ccut.edu.cn (H.L.); jrwu@jlu.edu.cn (J.-R.W.); haitao_wang@jlu.edu.cn (H.W.)

Abstract: Pesticide residues pose significant risks to human health and the environment, emphasizing the need for sensitive detection and analysis methods. Fluorescence-based sensors, particularly those utilizing aggregation-induced emission (AIE) fluorophores (AIEgens), have demonstrated exceptional performance in this area. This review summarizes key advancements in pesticide detection sensors based on AIEgens, detailing their luminescence mechanisms and fluorescence sensing principles. It explores various applications of AIEgens in fluorescence sensors, including organic small-molecule sensors, nanocomposite sensors, metal-organic framework sensors, supramolecular sensors, fluorescent porous organic polymer sensors, and lateral flow immunoassay sensors, with specific examples illustrating their detection mechanisms and performance. This review also discusses current challenges and future perspectives for the development of these sensors. We anticipate that this review will serve as a valuable and timely resource for researchers working to advance the development and application of AIEgens-based sensors in pesticide detection.

Keywords: aggregation-induced emission; pesticide detection; fluorescence sensing; supramolecular assembly

Citation: Zha, B.; Li, H.; Ren, S.; Wu, J.-R.; Wang, H. Aggregation-Induced Emission (AIE) Probes in Fluorescent Sensing: Progress and Applications for Pesticide Detection. *Appl. Sci.* **2024**, *14*, 8947. https://doi.org/10.3390/app14198947

Academic Editor: Paolo Prosposito

Received: 14 September 2024
Revised: 30 September 2024
Accepted: 2 October 2024
Published: 4 October 2024

1. Introduction

Pesticides, whether chemically synthesized or extracted from biological and other natural substances, are widely used to prevent and control diseases, insects, weeds, rodents, and other pests that threaten agriculture and forestry. They are also employed to regulate the growth of plants and insects. With the rapid growth in population and the intensification of global industrialization, pesticides have become an indispensable and important part of agricultural production [1,2]. The effective use of pesticides helps reduce pests and weeds, thus increasing crop product yield [3,4]. However, widespread use, coupled with high environmental persistence and human reliance, and the misuse of pesticides has led to significant residues in soil and water [5,6]. These residues pose serious risks by contaminating food, damaging ecosystems [7–9], and entering the human body through the food chain, potentially causing health issues and irreversible harm to organs such as the brain, heart, liver, and lungs [10,11]. Therefore, it is critical to develop sensitive methods for the detection and qualitative and quantitative analysis of pesticide residues to ensure human and environmental safety [12].

Several conventional techniques are employed for pesticide detection, including gas chromatography (GC) [13,14], mass spectrum (MS) [15], GC-MS [16–21], high-performance liquid chromatography [22,23], spectrophotometry, enzyme-linked immunosorbent assays, molecularly imprinted assays, nuclear magnetic resonance spectrometry [24], and electrochemical techniques [25,26]. While these methods provide high selectivity, sensitivity, and the ability to detect pesticides in complex samples, they also present several notable drawbacks. These include the high cost of instrumentation, lengthy sample preparation

procedures, complex sampling techniques, limited portability, and the need for specialized technicians to operate the equipment [27,28]. Additionally, large-scale analytical methods are often associated with significant manpower and time costs and strict testing conditions and are unsuitable for rapid quantitative detection or real-time, on-site analysis [29]. As a result, there is an urgent need for a simpler, faster, and more user-friendly method that can sensitively and selectively detect pesticide residues in the environment. Fluorescence detection offers a promising alternative, with advantages such as low detection limits, high sensitivity, ease of operation, and rapid response times.

Fluorescence detection methods offer several advantages, such as high sensitivity to target analytes, biocompatibility, and high photoluminescence quantum yield [30–32]. Over the past few decades, researchers have successfully employed these methods for the detection of a wide range of substances [33–38]. However, additional research is needed to improve the detection of pesticide residues in environmental settings, particularly in aqueous environments where most pesticide residues accumulate, creating a complex detection challenge. In aqueous environments, traditional fluorescent molecules tend to aggregate, resulting in the weakening or quenching of fluorescence, a phenomenon known as aggregation-caused quenching (ACQ). This significantly impairs the performance of fluorescence sensors for detecting pesticide residues [39]. To overcome this challenge, extensive research has been conducted, and one of the most notable breakthroughs is the concept of aggregation-induced emission (AIE), first proposed by Tang et al. [40]. Unlike the ACQ effect, AIE materials exhibit enhanced fluorescence in an aggregated state (e.g., at higher concentrations or in the solid state), providing a novel approach for developing fluorescence-based sensing and detection systems [41,42].

AIEgens (aggregation-induced emission fluorophores) [43] can emit bright and stable light due to their non-planar structure, which prevents π-π stacking interactions. This structure triggers non-radiative decay pathways and restricts molecular motion, enhancing their luminescent properties. Additionally, AIEgens exhibit several favorable characteristics, including a high signal-to-noise ratio, high sensitivity, high quantum yield, resistance to photobleaching, excellent biophysical stability, and cytocompatibility. As a result, AIEgens have found widespread application across diverse fields such as life sciences, materials science, physics, and inorganic chemistry, particularly as advanced functional materials when combined with other systems [44–46].

Based on the above analysis, this review provides a comprehensive summary of the research progress of AIEgens in fluorescence sensing for pesticide detection. We discuss the unique luminescence mechanism of AIE materials and the design strategy for developing AIEgens-based fluorescence sensors. By surveying the limitations and drawbacks of existing pesticide detection methods, we emphasize the design principles and practical applications of AIEgens when combined with other functional materials for detection (Scheme 1). Finally, this review addresses the challenges associated with AIE@functional materials in improving detection efficiency and accuracy and proposes potential directions for future development.

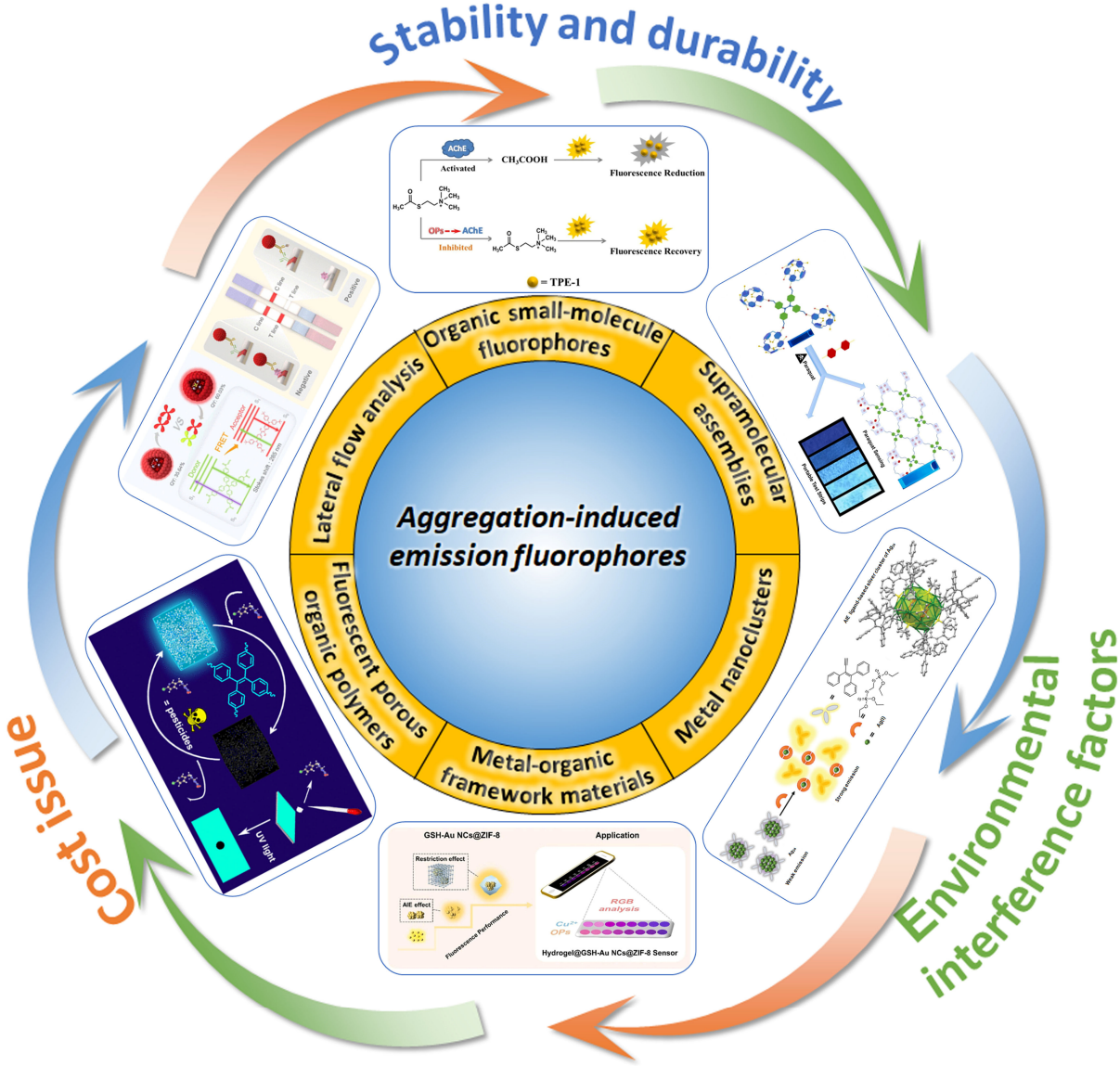

Scheme 1. Sensors based on AIEgens for pesticide detection.

2. The Luminescence Mechanism of AIEgens and Detection Mechanisms Based on AIEgens Fluorescence Sensing

2.1. The Luminescence Mechanism of AIEgens

Common organic fluorescent dyes used in chemical sensor detection, such as rhodamine, fluorescein, and indocyanine green, are known for their high fluorescence quantum yields and sensitivity. However, they also exhibit limitations, including short Stokes shifts, poor photostability, and insufficient water solubility, which hinder their practical applications. The introduction of AIE molecules has transformed the understanding of photoluminescent properties in materials.

The luminescence of AIE materials is widely attributed to the restriction of intramolecular motion (RIM), which encompasses both intramolecular rotation (RIR) and intramolecular vibration (RIV) [47–54]. In a good solvent, AIEgens typically experience nonradiative decay as energy is dissipated through these intramolecular motions. However, when a poor solvent is introduced, AIEgens aggregate, which suppresses intramolecular motion and shifts the energy dissipation pathway towards radiative decay. Unlike conventional organic fluorescent molecules, the aggregated state of AIEgens inhibits intermolecular stacking, resulting in high fluorescence quantum yields and exceptional photostability in both aggregated and solid states.

Currently, AIEgens based on the classical RIM mechanism include tetraphenylethylene (TPE), hexaphenylsilole, cyanostilbene, and 9,10-distyrylanthracene, all of which exhibit remarkable AIE characteristics and excellent luminescence controllability. [55–57] These materials are easy to synthesize and functionalize, making them valuable for applications in pesticide detection. Furthermore, "irregular AIEgens" [58] and natural AIEgens [59] have emerged, broadening the scope of AIE materials. Irregular AIEgens, which include nanodots, metal nanoparticles, and non-conjugated polymers, lack rotating aromatic moieties but still demonstrate superior optical properties, multifunctionality in surface modification, unique surface plasmon resonance, and electrical catalysis. These materials hold significant potential for detecting pesticide residues [60,61]. Natural AIEgens, derived from sustainable biomass materials, offer advantages such as sustainability, low cost, biocompatibility, and ease of preparation. They particularly excel in pest and disease management [62]. Overall, advancements in molecular engineering have resulted in diverse structural forms of AIE molecules, providing a robust foundation for designing innovative AIE probes.

2.2. Detection Mechanism Based on AIEgens Fluorescence Sensing

AIEgens-based fluorescent sensors offer a diverse range of detection mechanisms, depending on the chemical structure and optical properties of the target analyte [63–68]. The main detection mechanisms include the following:

(i) Chemical interaction-based detection: These sensors are equipped with chemically reactive groups capable of protonation or deprotonation. Interactions between the sensor and the target molecule can alter the optical properties or solubility of the mixture, resulting in a detectable signal. (ii) Interaction-based detection: This mechanism involves interactions such as metal-ligand coordination, electrostatic bonding, hydrogen bonding, and π-π interactions. These interactions can induce changes in the optical properties or effects between the sensor and the target substance, facilitating detection. (iii) Photophysical process-based detection: This approach relies on changes in photophysical processes in the presence of the target substance. Key processes include the following: (1) intramolecular charge transfer (ICT)—involves electron-donating and electron-accepting groups. Interaction with the target alters the electronic properties of these groups, affecting fluorescence; (2) photoinduced electron transfer (PET)—the interaction between electron-rich and electron-deficient components modifies the highest occupied molecular orbital (HOMO) and lowest unoccupied molecular orbital (LUMO) energies, leading to changes in fluorescence; (3) Förster resonance energy transfer (FRET)—requires physical proximity between donor and acceptor molecules, with the emission spectra of the donor overlapping with the absorption spectra of the acceptor; (4) excited state intramolecular proton transfer (ESIPT)—excitation causes electron delocalization and hydrogen proton transfer through intramolecular hydrogen bonding, resulting in structural transitions and reciprocal isomerism; (5) internal filtering effect (IFE)—in the system, there must be a substance that can absorb excitation light or emitted light, and the absorption spectrum of this substance has an overlapping part with the excitation spectrum of the fluorescent substance. (iv) Biomolecular detection: This method includes lateral flow immunoassay devices or the conjugation of biomolecules (such as peptides, antigens, and antibodies) to AIEgens. This approach is used for the specific detection and identification of analytes through biomolecular interactions.

3. Application of AIEgens in the Detection of Pesticide Residues in Fluorescence Sensors

Based on the detailed mechanisms outlined above, we have categorized the application of AIEgens in fluorescence sensors for pesticide detection into several key areas: AIE-small molecules [27,69–71], AIE-nanocomposites [28,72–75], AIE-organic metal frameworks [76–78], AIE-supramolecules [79–82], AIE-porous organic polymers [83–85], and AIE-lateral flow immunoassays [86]. This section highlights the distinct advantages of AIEgens over traditional fluorescent groups, focusing on their integration with various functional materials to enhance optical properties, broaden detection ranges, and enable

visual identification of pesticide residues. Table 1 summarizes the AIE sensing platforms that have been developed for these applications.

Table 1. Summary of sensing type, LOD, and mechanism of AIE-type sensors for pesticide detection.

Sensor Type	Sensor	Analyte	LOD	Detection Range	Sensing Type	Mechanism	Ref.
Small molecules	A1	Organophosphorus pesticides	0.008 mg/L	0.009–22.5 mg/L	Turn-on	Specific recognition and chemical interaction	[27]
	A2	Carbamate pesticides	27.8 ng/mL	0 μg/mL–50 g/mL	Turn-off	Specific recognition and chemical interaction	[69]
	A3	Trifluralin	6.28 μg/L	20–90 μg/L	Turn-off	Photophysical quenching process	[70]
	A4	Paclobutrazol	9.3×10^{-8} M	2×10^{-7}–9×10^{-6} M	Turn-on	Photophysical change process and solubility change	[71]
Nanocomposites	A5	Organophosphorus pesticides	0.4 μg/L (Fluorescence) 0.09 μg/L (colorimetric)	1–50 mg/L (Fluorescence) 0.1–50 mg/L (colorimetric)	Turn-off	Specific recognition and molecular self-assembly	[72]
	A6	Paraoxon	0.38 ng/mL	0.8–60 ng/mL	Turn-off	Specific recognition and molecular self-assembly	[73]
	A7	Ethion	0.96 mM	0–50.0 mM	Turn-on	chemical interaction	[74]
	A8	Organophosphorus pesticides	1 μg/L	1–100 μg/L	Turn-off	Specific recognition	[75]
	A9	/	/	/	/	Specific recognition	[28]
Organic metal frameworks	A10	Imidacloprid (IM), Thiamethoxam (TH) pesticides	5.57 μg/L (IM) 0.98 μg/L (TH)	1–20,000 μg/L	/	solubility change	[76]
	A11	Methyl parathion	1.3×10^{-3} mg/L	0.1–5 mg/L	Turn-off	Noncovalent interaction	[77]
	A12	Glyphosate	0.28 nM	0–100 nM	Turn-off	Specific recognition and chemical interaction	[78]
Supramolecular assemblies	A13	Carbaryl	0.007 μg/L	0.02–2.00 μg/L	Ratiometric	Specific recognition and photophysical change process	[79]
	A14	Fipronil	0.05 μM	0–1 μM	Ratiometric	Specific recognition and photophysical change process	[80]
	A15	Paraquat	154.1 nM	0–120 μM	Turn-on	Noncovalent interaction	[81]
	A16	Paraoxon methyl	501 μM	0–45 mM	Turn-on	Specific recognition and molecular self-assembly	[82]
Porous organic polymers	A17	Trifluralin, Isopropalin, Glyphosate, Fenitrothion, Imidacloprid, Cyfluothrin	/	/	Turn-off	Photophysical quenching process	[83]
	A18	Imidacloprid, Cyfluothrin, Triflumizole, Lambda-cyhalothrin	30–1100 ppb (A18-1) 83–4207 ppb (A18-2)	/	Turn-off	Photophysical quenching process	[84]
	A19	Imidacloprid, Triflumizole, Lambda-Cyhalothrin, Acetamiprid and Indoxacarb	28–2570 ppb (A19-1) 0.13–2.54 ppm (A19-2)	/	Turn-off	Photophysical quenching process	[85]
Lateral flow immunoassays	A20	Chlorothalonil	1.2 pg/mL	0–500 ng/mL	Turn-off	Specific recognition	[86]

3.1. Detection of Pesticides Using Organic Fluorescent Small-Molecule Sensors Based on AIEgens

Organic small-molecule sensors utilizing AIEgens rely on the AIE properties of these compounds. By selecting AIEgens with specific optical properties or those that interact with pesticide molecules and by designing and synthesizing these molecules to tailor their luminescence properties and sensitivity, these sensors achieve high sensitivity and selective detection of pesticides.

For instance, Liu et al. synthesized tetraphenylethylene derivatives TPE-1 (A1-1) and TPE-2 (A1-2) with different aldehyde groups (Figure 1a) [27]. Both probes exhibited notable AIE characteristics, but A1-2 demonstrated lower quantum yield and sensitivity to pH compared to A1-1. Consequently, A1-1 was selected for detecting organophosphorus pesticides (OPs) (Figure 1b,c). The detection mechanism of A1-1 is based on the irreversible inhibition effect of OPs on the activity of acetylcholinesterase (AChE). This inhibition reduces the hydrolysis of acetylthiocholine iodide (ATCh) to acetic acid, diminishing the protonation of A1-1 and thereby initiating a fluorescence signal for OP detection (Figure 1d). Essentially, the presence of OPs inhibits AChE, decreases acetic acid production, reduces

A1-1 protonation, and restores fluorescence, enabling "turn-on" detection of OPs. Practical applicability was further validated through standard addition experiments in real water samples, with recoveries ranging from 98% to 112%, highlighting the potential of A1-1 as an effective pesticide detection probe.

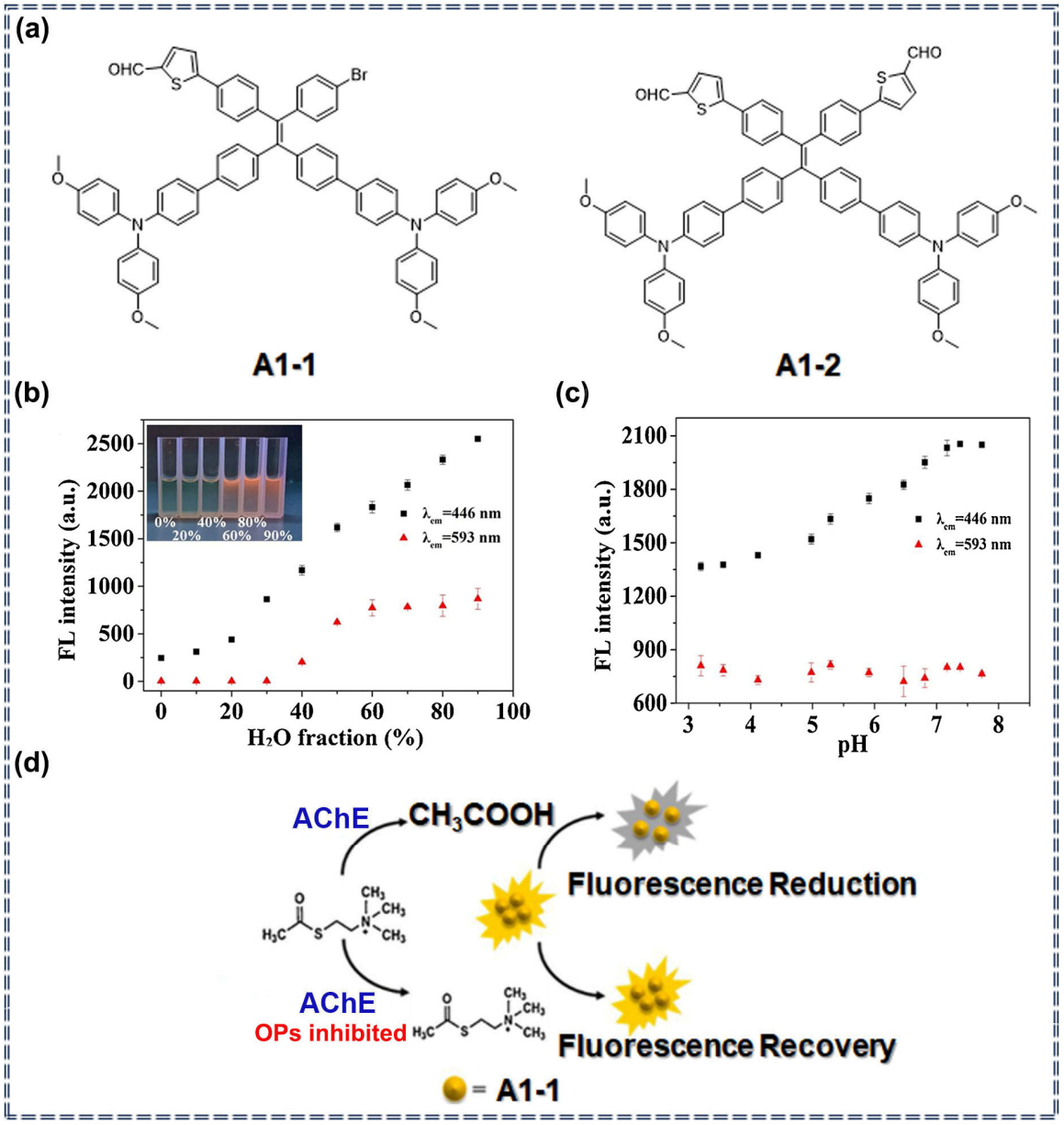

Figure 1. (**a**) Structures of A1-1 and A1-2; (**b**) Fluorescence intensity at emission wavelengths of 446 nm and 593 nm for different water contents. Inset: Fluorescence images at varying water fractions (0%, 20%, 40%, 60%, 80%, and 90%); (**c**) Fluorescence intensity of A1-1 at different pH values at 446 nm and 593 nm. (λex = 365 nm); (**d**) Detection mechanism of A1-1 for OPs. (Reproduced with permission from ref. [27]. copyright 2019 Elsevier).

Shen et al. designed and synthesized the probe CBZ-FP (A2) based on a chromophore of AIE fluorescent protein (Figure 2a inset) [69]. This probe has a large Stokes shift, enhanced fluorescence, and low background noise (Figure 2a,b). It can indirectly detect carbamates by assessing the activity of carboxylesterases (CESs). The ester group in A2 serves as a specific reactive substrate for CESs. The reaction of the ester group with CESs increases the carboxyl group's electronegativity, leading to enhanced fluorescence. However, the presence of carbamate pesticides inhibits carboxylesterase 1 (CES1), preventing

the hydrolysis reaction in A2 and resulting in reduced fluorescence intensity, thus enabling the detection of carbamates (Figure 2c). Probe A2 achieved a limit of detection (LOD) of 27.8 ng/mL for carbamate pesticides, demonstrating its effectiveness and providing a useful method for pesticide detection.

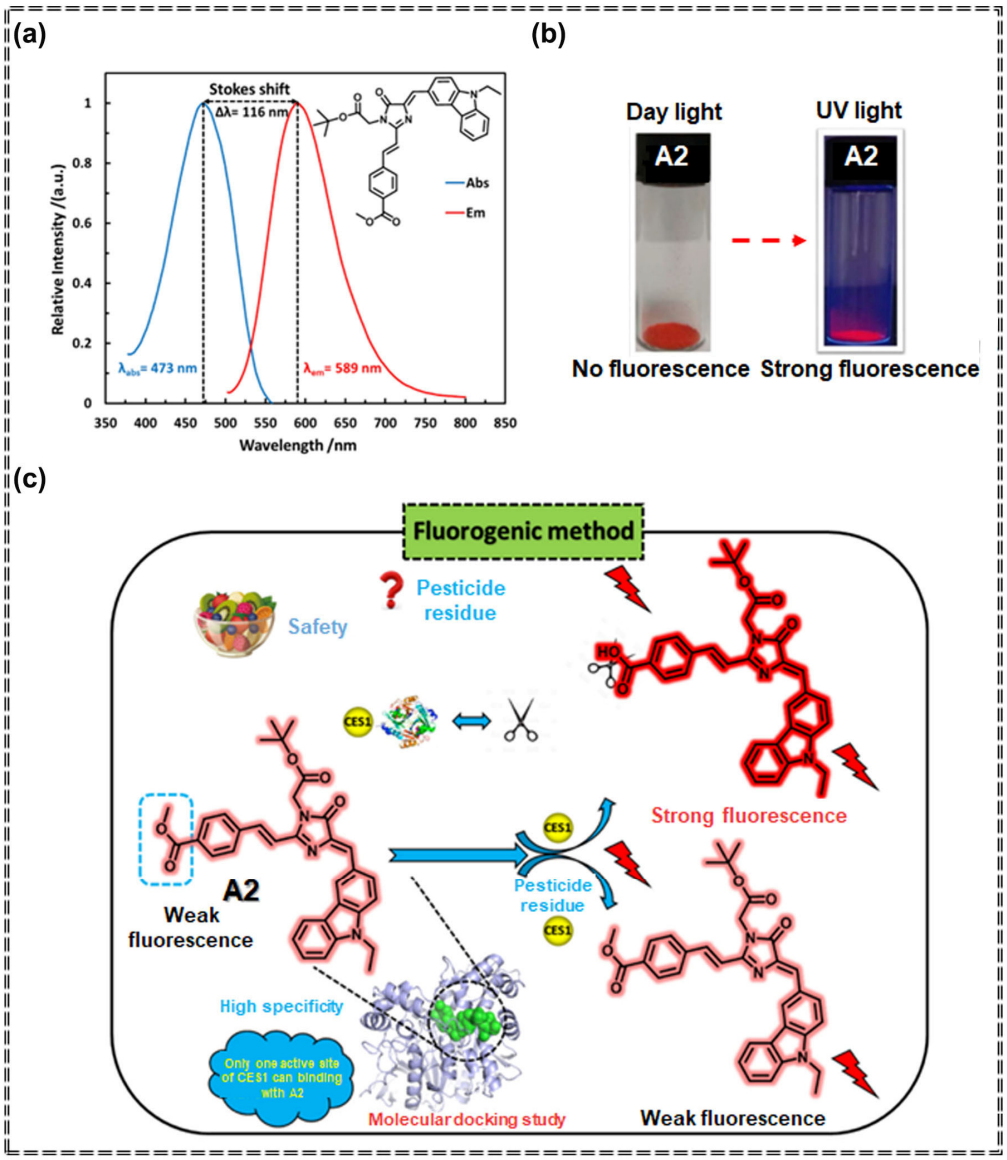

Figure 2. (**a**) Relative absorbance and fluorescence spectra of A2 (10 μM) in CH_3CN/PBS buffer (v/v = 1/1) at 25 °C. Inset: Structure of compound A2; (**b**) Fluorescence images of A2 under UV light and daylight; (**c**) Schematic illustration of the binding mechanism for A2 in the detection of carboxylesterases and carbamates. (Reproduced with permission from ref. [69]. copyright 2021 Elsevier).

Zhang et al. synthesized the AIEgens-based small-molecule fluorescent probe TPETPy (A3) through a one-step reaction (Figure 3a) [70]. The fluorescence properties of A3 were investigated in THF/H_2O mixed solvents with varying water fractions, and its sensing performance for trifluralin was evaluated (Figure 3b,c). The detection mechanism of trifluralin using probe A3 relies on the PET mechanism. Upon ultraviolet light excitation, A3 and trifluralin exhibit well-matched energy levels, facilitating effective electron transfer from the excited-state A3 molecule to the ground-state trifluralin molecule. This electron transfer results in the fluorescence quenching of A3, enabling the detection of trifluralin. Additionally, a smartphone-integrated sensing platform was developed based on A3 for trifluralin detection, which allowed for real-time output of the RGB (red, green, and blue)

values in the fluorescence mode (Figure 3d). This platform enabled real-time and on-site quantitative monitoring of trifluralin, and its practical applicability was confirmed through standard addition experiments.

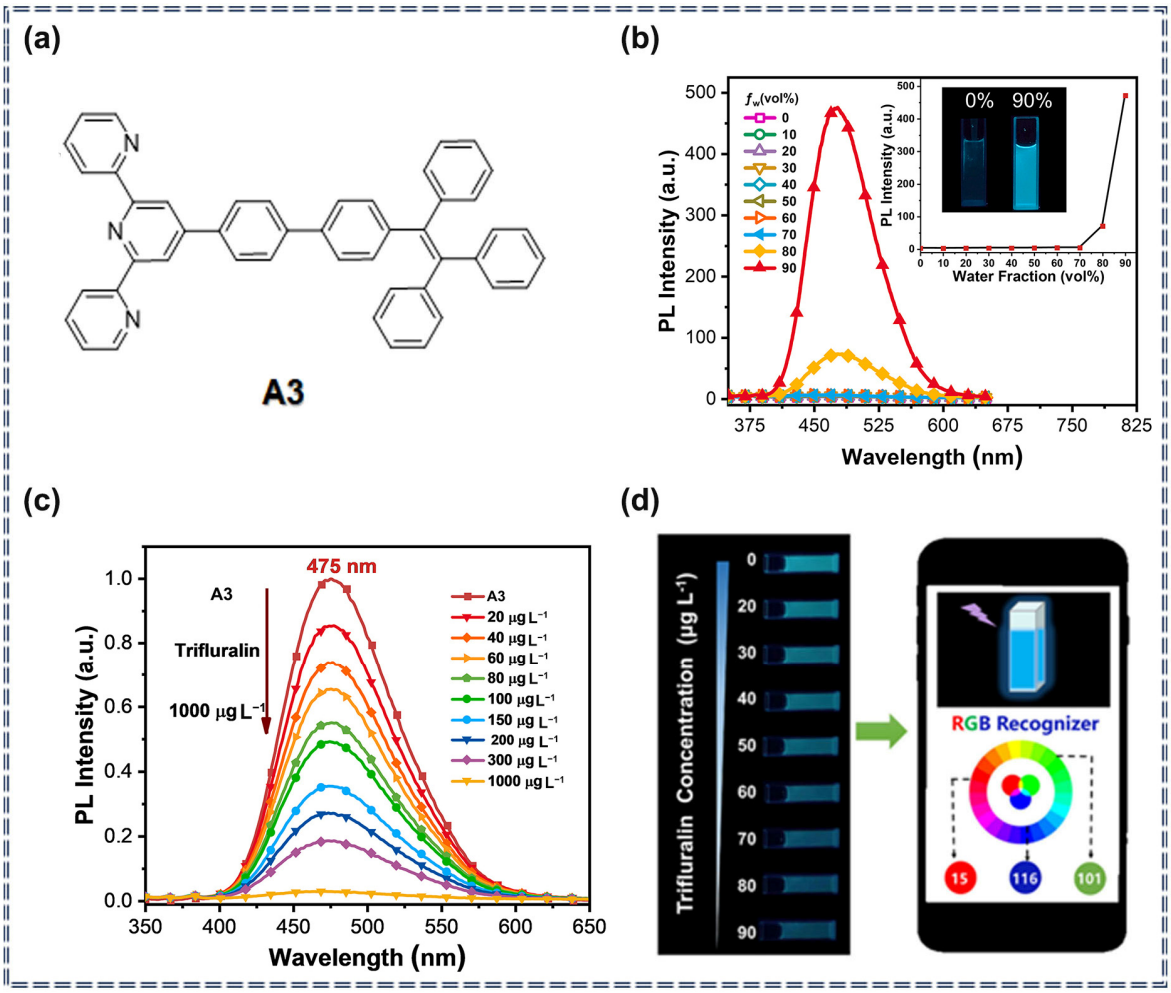

Figure 3. (**a**) Structure of compound A3; (**b**) PL spectra of A3 in THF/water mixtures with varying water fractions. Inset: Variation of PL intensity with different water contents, with corresponding photos showing A3 solutions in THF/water mixtures with 0% and 90% water content; (**c**) Fluorescence spectra of A3 (1 μM) in the presence of increasing concentrations of trifluralin (20–1000 μg L^{-1}); (**d**) Fluorescence images of A3 upon the addition of trifluralin (0–90 μg L^{-1}), along with a schematic diagram showing the real-time recognition of RGB values of the A3 probe using a smartphone color recognizer. (Reproduced with permission from ref. [70]. copyright 2024 Elsevier).

Yang et al. synthesized the AIE-active small-molecule probe TPS (A4) using benzoyl, aniline, and *p*-acetamidobenzaldehyde as starting materials (Figure 4c) [71]. A4 exhibits a pronounced AIE effect and demonstrates significant "turn-on" and "color change" fluorescence responses to paclobutrazol, with a LOD of 9.3×10^{-8} M (Figure 4a,b). The detection mechanism involves the formation of a new aggregation effect when A4 interacts with paclobutrazol through hydrogen bonding, which reduces the energy gap and results in enhanced fluorescence (Figure 4c). To assess the practical applicability of A4 for simple, real-time, and in situ detection of paclobutrazol in agricultural production and daily life, its selective detection capability was evaluated in real sample environments (Figure 4d,e). The results confirmed the high effectiveness of A4, highlighting its potential for practical pesticide detection applications.

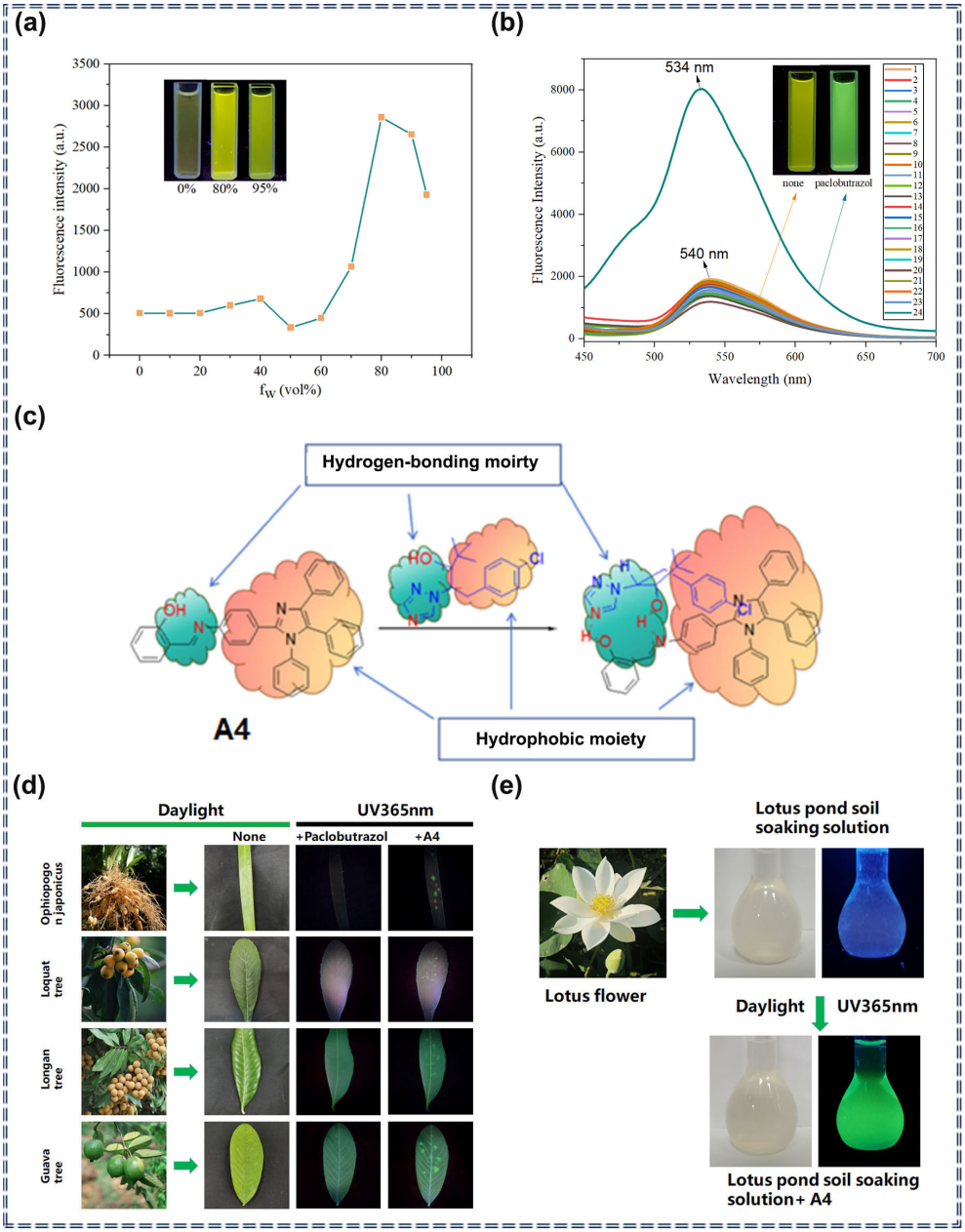

Figure 4. (**a**) Fluorescence intensity of A4 as a function of water content. Inset: Fluorescence photographs of A4 in water fractions of 0%, 80%, and 95%; (**b**) Fluorescence spectra of A4 (1.0×10^{-5} M) in DMSO/H_2O (5/95) solution with various pesticides and metal ions (1.0×10^{-5} M each, λex = 380 nm). The labeled peaks correspond to: 1 = A4, 2 = 1 + Na^+, 3 = 1 + K^+, 4 = 1 + Ca^{2+}, 5 = 1 + Mg^{2+}, 6 = 1 + Al^{3+}, 7 = 1 + thiamethoxam, 8 = 1 + hexazinone, 9 = 1 + fluroxypyr, 10 = 1 + clopyralid, 11 = 1 + carbendazim, 12 = 1 + quizalofop-pethyl, 13 = 1 + glufosinate-ammonium, 14 = 1 + N-(Phosphonomethyl) glycine 2-propylamine, 15 = 1 + mancozeb, 16 = 1 + thiophanate-methyl, 17 = 1 + sulfometuron-methyl, 18 = 1 + triclopyr 2-butoxyethyl ester, 19 = 1 + triadimefon, 20 = 1 + monosultap, 21 = 1 + molosultap, 22 = 1 + metaldehyde, 23 = 1 + bromoxynil octanoate, 24 = 1 + paclobutrazol. Inset: Photographs showing A4 alone and A4 with paclobutrazol; (**c**) Proposed sensing mechanism of A4 for paclobutrazol detection; (**d**) Photographs of real leaf samples (*Ophiopogon japonicus*, loquat tree, longan tree and guava tree) treated with paclobutrazol and A4, under daylight and UV light (365 nm). The samples were sprayed with a solution of paclobutrazol followed by A4; (**e**) Application on A4 (1.0×10^{-5} M) for the detection of paclobutrazol in lotus pond soil soaking solution samples. (Reproduced with permission from ref. [71]. copyright 2024 Elsevier).

The studies above employ fluorescent probes made from organic small molecules with specific structures. Using mechanisms like AIE and PET, these probes achieve highly sensitive and selective detection of pesticides, including OPs, carbamates, and trifluralin. The development of portable detection platforms for use in complex environments further highlights the potential of composite materials combining AIEgens and organic small molecules for effective pesticide detection.

3.2. Detection of Pesticides by Nanocomposite Sensors Based on AIEgens

Combining AIEgens with nanocomposites can utilize the unique fluorescence characteristics of AIEgens and the special properties of nanocomposites to achieve high-sensitivity and high-selectivity pesticide detection [87,88]. The detection mechanisms of such sensors generally fall into three types: (i) Fluorescence change of AIEgens: When pesticides interact with AIEgens within the nanocomposite, they may alter the aggregation state of AIEgens, leading to changes in fluorescence intensity or wavelength. These changes can be used to quantitatively or qualitatively detect pesticides by monitoring the fluorescence signal. (ii) Nanomaterial properties: Nanocomposites can enhance the fluorescence of AIEgens through various mechanisms. For instance, the surface plasmon resonance effect of metal nanoparticles can amplify AIEgens' fluorescence, while the conductivity of carbon nanomaterials can be utilized in electrochemical sensors. Pesticides are detected by measuring changes in current or potential. (iii) Multiple signal detection: By combining the fluorescence signal of AIEgens with other properties of nanomaterials (such as resistance or capacitance), multiple signal detection can be achieved. This approach improves the accuracy and reliability of pesticide detection.

For example, Liu et al. developed the MnO_2-AuNCs-SiO_2 composite material (A5) through the self-assembly of Au nanoclusters (AuNCs), silica nanoparticles (SiO_2 NPs), and manganese dioxide (MnO_2) nanosheets (Figure 5a) [72]. This composite was used for dual-mode fluorescence and colorimetric detection of OPs. The detection mechanism involves the electrostatic adsorption of weakly fluorescent **AuNCs** onto the surface of SiO_2, which enhances their AIE properties and amplifies the fluorescence signal. In the presence of alkaline phosphatase (ALP), sodium L-ascorbyl-2-phosphate (AAP) is dephosphorylated to produce ascorbic acid (AA). AA decomposes MnO_2, causing the solution to change from brown to colorless, thereby restoring the fluorescence of AuNCs-SiO_2. When OPs, such as acephate, are present, they inhibit ALP activity, reducing AA production and preventing the complete decomposition of MnO_2. This results in weakened fluorescence recovery and increased absorbance. The practical performance of A5 was demonstrated by applying it to fresh vegetables and test papers for in situ imaging (Figure 5b,c) and visual semi-quantitative detection of OPs, showcasing the significant potential of AIEgens-based nanocomposites for practical applications.

Chi et al. synthesized an amphiphilic polymer (PTD) containing AIE-active fluorophores and quaternary ammonium salt groups via free radical copolymerization, which self-assembled into AIE-active nanoparticles (A6) (Figure 6a) [73]. A sensor A6@AuNPs for highly sensitive OP detection was developed using A6 as the fluorescence signal reporter and gold nanoparticles (AuNPs) as the nanoquencher (Figure 6b). Electrostatic interactions between A6 and AuNPs caused FRET, which quenched the fluorescence of A6. In the presence of ATCh, AChE hydrolyzed it to produce thiocholine. Thiocholine then competitively bound to AuNPs, preventing FRET and thereby enhancing fluorescence However, when OPs are present, the activity of AChE is effectively inhibited, resulting in the absence of thiocholine production. The inhibition of AChE activity leads to the obstruction of the FRET effect, and no enhanced fluorescence can be detected, thereby achieving the detection of OPs (Figure 6c). This work advances high-performance AIE nanoparticles and broadens their application scope.

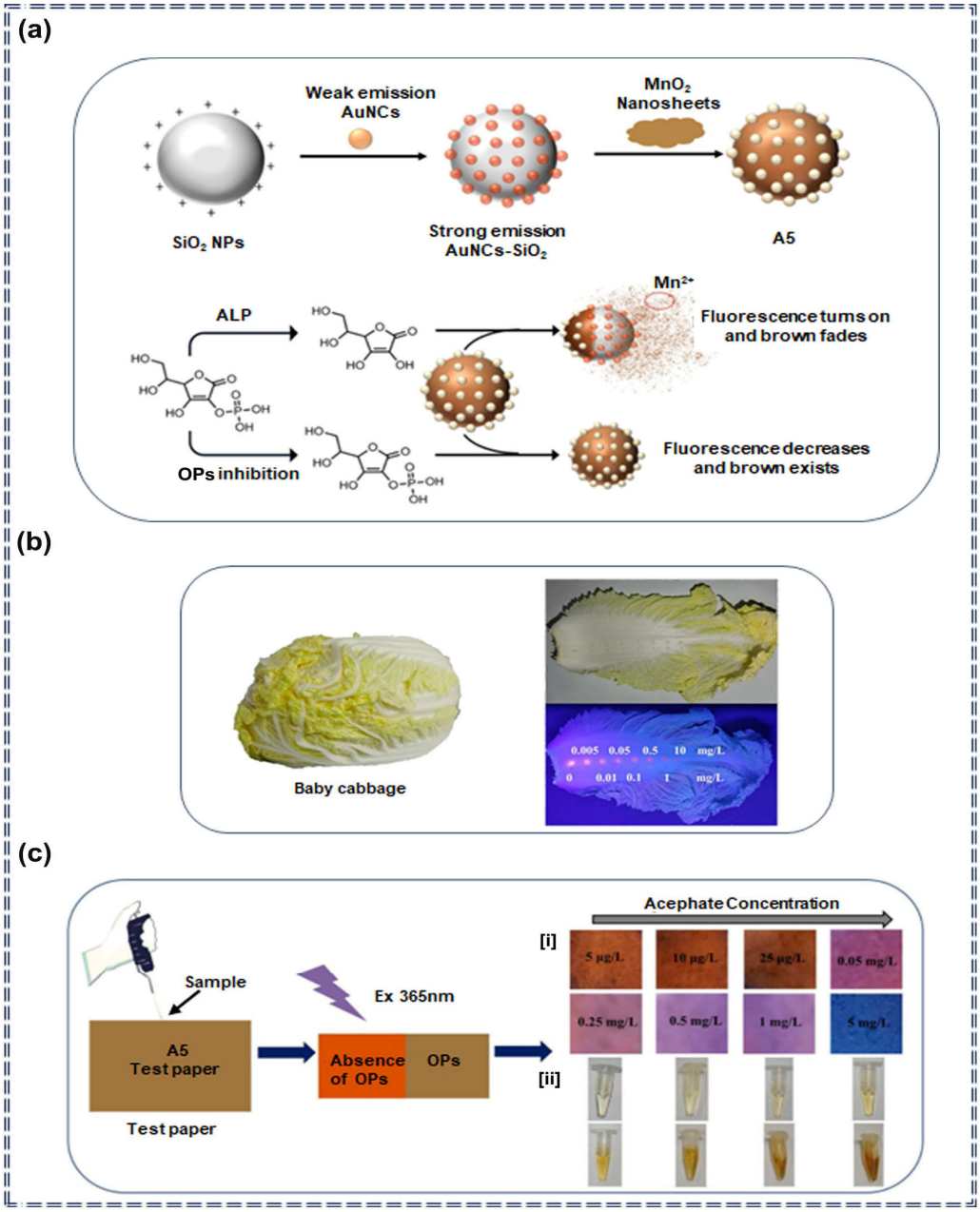

Figure 5. (**a**) Schematic illustration of the detection mechanism for OPs using A5; (**b**) Visible imaging of acephate at various concentrations on the surface of fresh cabbage; (**c**) Color changes on A5 test paper [i] and in an A5 solution in a tube [ii] at different acephate concentrations, with the presence of ALP and AAP. (Reproduced with permission from ref. [72]. copyright 2020 Elsevier).

Zang et al. prepared a silver cluster (Ag_{24}, denoted as A7) by combining the AIE-active ligand 1,1,2-triphenyl-1-buten-3-yne (TPBA) with silver ions, which was used to detect ethion among OPs [74]. TPBA exhibits AIE characteristics. Emitting cyan fluorescence in both its aggregated and solid states. The cluster A7 consists of twelve TPBA ligands, eight tert-butylthiol ligands, and two encapsulated NO ions (Figure 7a). The presence of sulfur in OPs, such as ethion, can effectively disrupt A7 and release the AIE-active fragments. This disruption leads to a "turn-on" fluorescence emission change, enabling the successful detection of ethion (Figure 7b). A7 demonstrated high selectivity for ethion, with a LOD of 0.96 mmol/L.

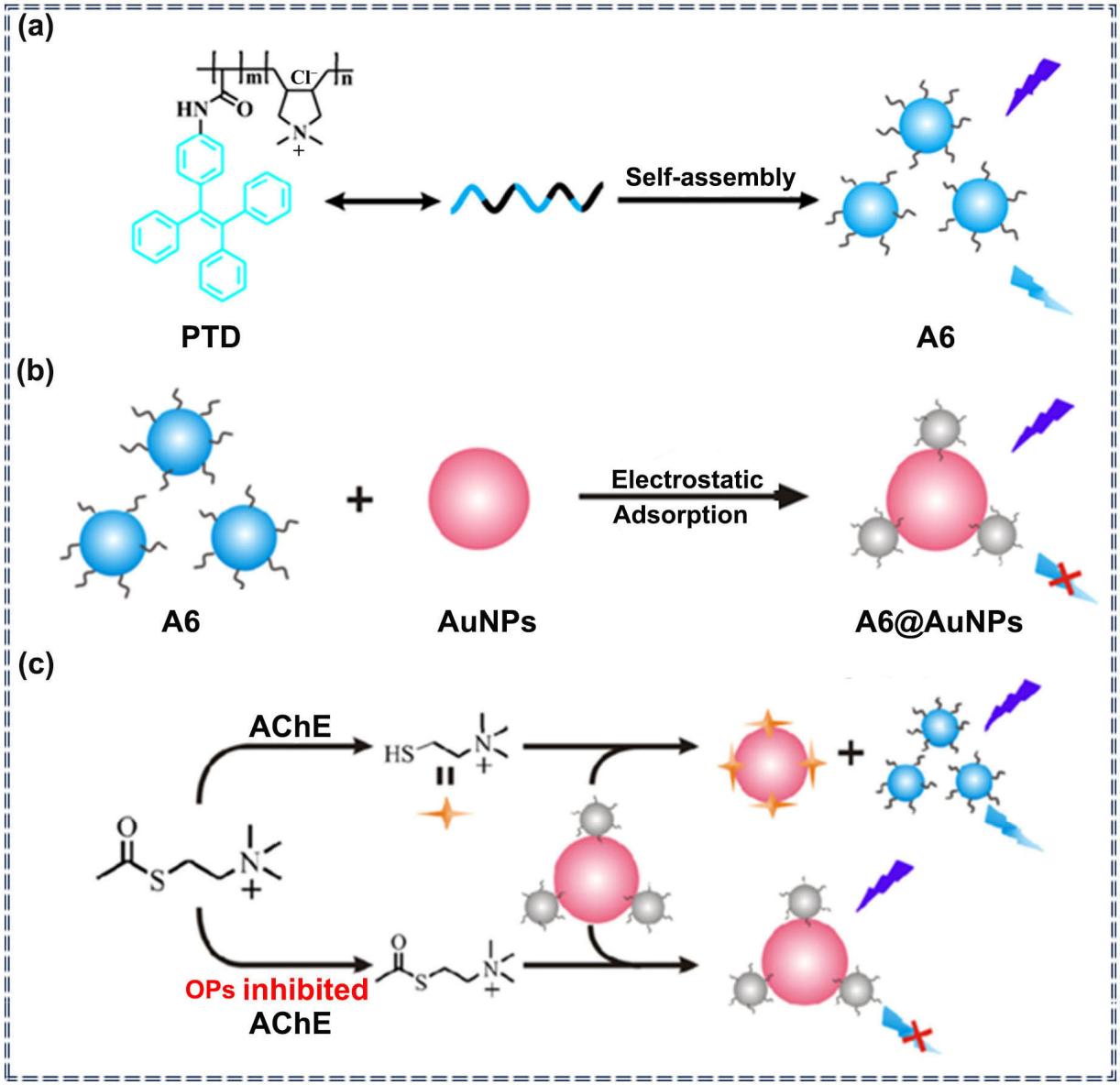

Figure 6. (**a**) Schematic representation of A6 fabrication through the self-assembling strategy; (**b**) Schematic illustration of the interaction between A6 and AuNPs; (**c**) Schematic of A6@AuNPs biosensors for highly sensitive detection of AChE and OPs. (Reproduced with permission from ref. [73]. copyright 2019 American Chemical Society).

Xue et al. developed a fluorescent sensor (TPE-SiO_2-MnO_2, denoted as A8) for OP detection, combining tetraphenylethylene derivative (BSPOTPE), SiO_2 nanoparticles (SiO_2 NPs), and MnO_2 nanosheets (Figure 8a) [75]. BSPOTPE and SiO_2 NPs, being oppositely charged, form a stable electrostatic assembly and emit strong fluorescence. However, the presence of MnO_2 nanosheets quenches the fluorescence of the BSPOTPE-SiO_2 nanocomposites. When thiocholine (TCh) is present, it decomposes the MnO_2 nanosheets, restoring the fluorescence of the BSPOTPE-SiO_2 nanocomposites. This interaction enables the detection of OPs through their inhibitory effect on AChE, which is translated into a "turn-off" fluorescence signal. To streamline the detection process, the researchers also created a fluorescent test strip for OP measurement (Figure 8b). This "switchable" fluorescent sensor shows great potential for in-situ and field inspections.

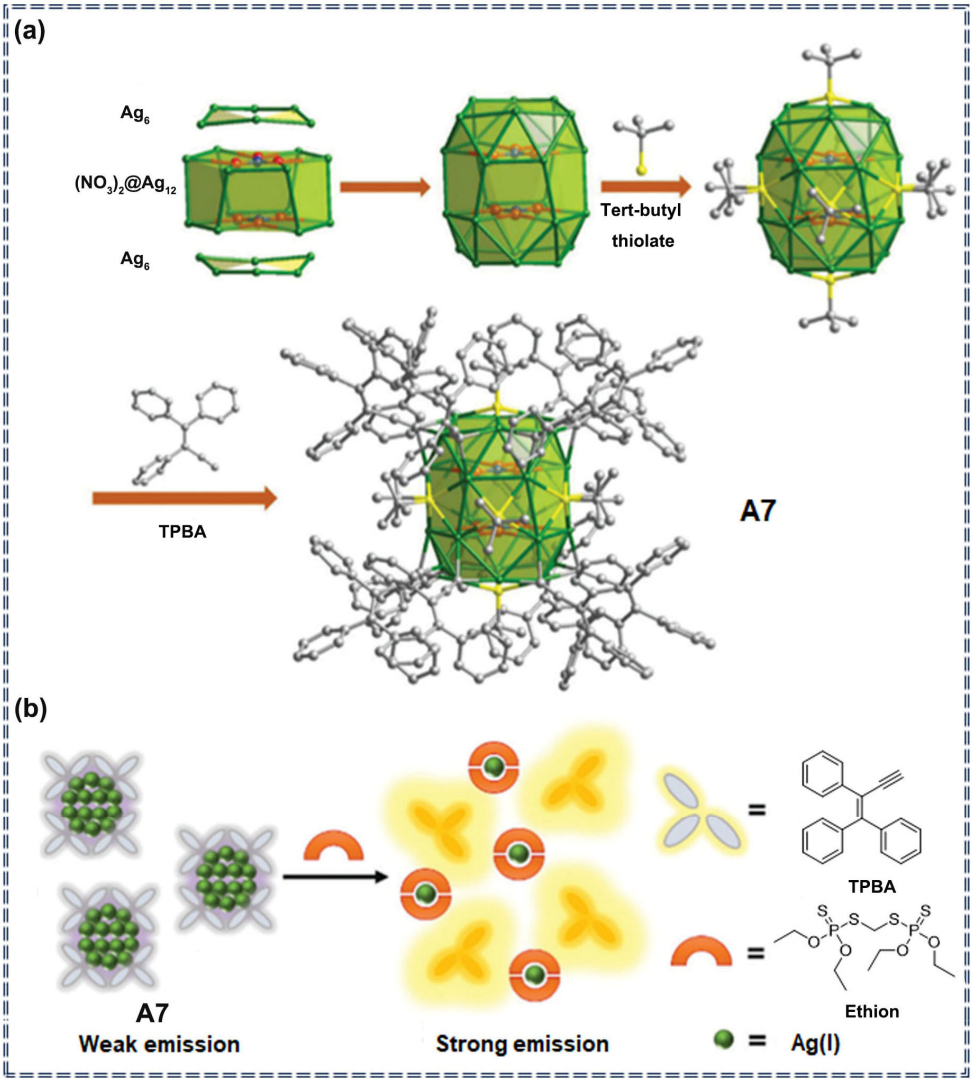

Figure 7. (**a**) The structure and coordination mode of the A7 cluster; (**b**) Proposed mechanism for the interaction between A7 and ethion. (Reproduced with permission from ref. [74]. copyright 2021 Chinese Chemical Society).

Yin et al. developed a TPE-based AIE star polymer (TPE-Pn), with the optimized polymer TPE-P50 (A9) being utilized as a multifunctional nanocarrier for simultaneous delivery of the pesticide dinotefuran (DIN) and double-stranded RNA (dsRNA) [28]. The A9 polymer features a TPE core, which is hydrophobic, and poly(2-(dimethylamino) ethyl methacrylate) (PDMAEMA) arms, which are hydrophilic (Figure 9a). The positively charged PDMAEMA arms facilitate the formation of hydrogen bonds and electrostatic interactions with DIN and dsRNA, resulting in the dsRNA/DIN/A9 complex (Figure 9b). The combination of the twisted TPE core and the positively charged PDMAEMA arms enhances the encapsulation of DIN and dsRNA, significantly improving the co-loading efficiency of these agents. This complex effectively facilitates the uptake and delivery of DIN and dsRNA to target pests, resulting in enhanced pest control. The loading efficiency of DIN using A9 was increased by 28% compared to commercial pesticides. By incorporating AIEgens, this approach not only improves the co-delivery efficiency of the drug and genetic material but also provides a new strategy for synergistic pest control, overcoming the limitations of traditional chemical and genetic insecticides.

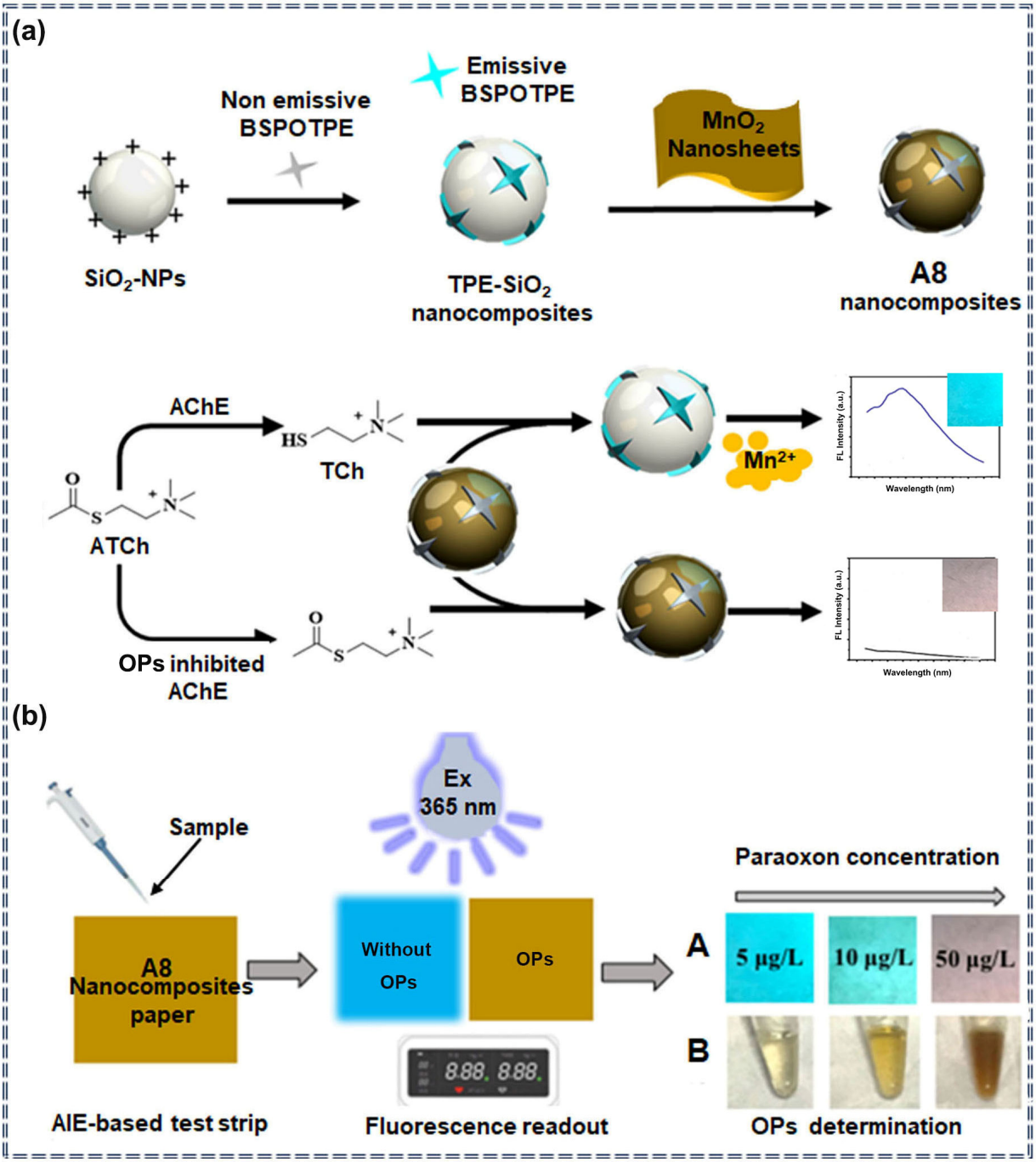

Figure 8. (**a**) Schematic illustration of the sensing mechanism for OPs using the A8 nanocomposites; (**b**) Detection of paraoxon with the A8 nanocomposites test paper strip. (Reproduced with permission from ref. [75]. copyright 2019 Elsevier).

All the aforementioned studies utilize fluorescent sensors designed with AIE molecules and nanomaterials that possess unique properties, such as AIE polymers, nanocomposites, and silver clusters. By utilizing various mechanisms—including AIE characteristics, FRET, IFE, and enzymatic reactions—these sensors achieve highly sensitive and selective detection or imaging of pesticides. Notably, some studies have developed portable detection platforms and conducted practical applications, specifically examining the interactions between sensors and pesticide molecules. These findings underscore the feasibility and significant application potential of integrating AIEgens with nanomaterials for effective pesticide detection.

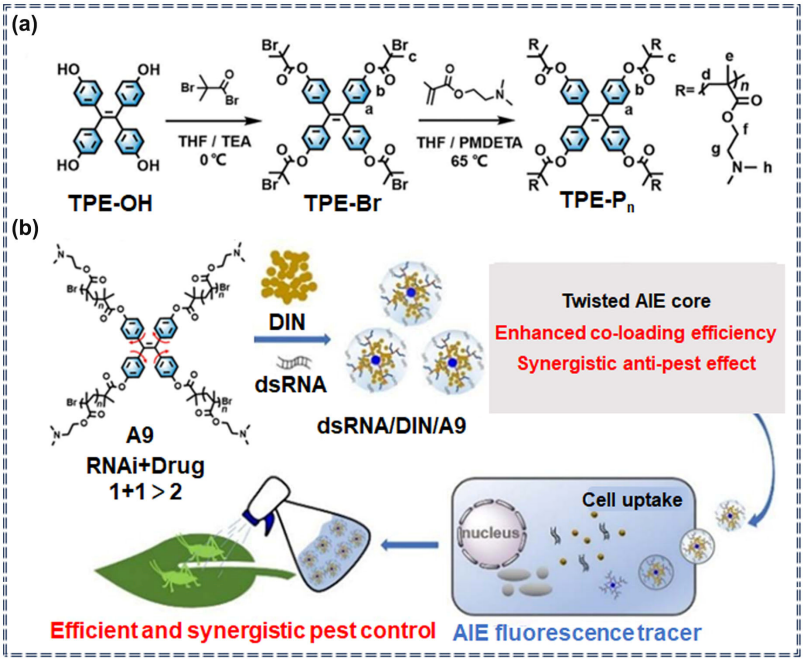

Figure 9. (**a**) Synthetic route of TPE-Pn; (**b**) Schematic illustration of the preparation of the dsRNA/DIN/A9 complex for enhanced co-loading of pesticides and synergistic pest control. (Reproduced with permission from ref. [28]. copyright 2023 Chinese Chemical Society).

3.3. Detection of Pesticides by Metal-Organic Framework Sensors Based on AIEgens

Combining AIEgens with metal-organic frameworks (MOFs) for pesticide detection can enhance selectivity and stability and enable diverse detection modes through functionalization such as fluorescence, colorimetry, and electrochemistry [89].

For example, Jiang et al. developed the luminescent MOF UiO-66-NH_2 (A10), which effectively detects imidacloprid (IM) and thiamethoxam (TH) by evaluating its selectivity, anti-interference capability, and fluorescence sensing mechanism (Figure 10) [76,90]. In the presence of IM or TH, A10 forms aggregates, increasing particle sizes to 63,628.57 nm (IM) and 77,068.65 nm (TH) and altering zeta potentials to −14.39 mV (IM) and −14.31 mV (TH). The LOD for A10 are 5.57 μg/L for IM and 0.98 μg/L for TH. A10 also successfully detected IM and TH in real juice samples, with recoveries between 85% and 116%. This study highlights the potential of A10 for rapid and selective sensing of pesticides in environmental and food matrices.

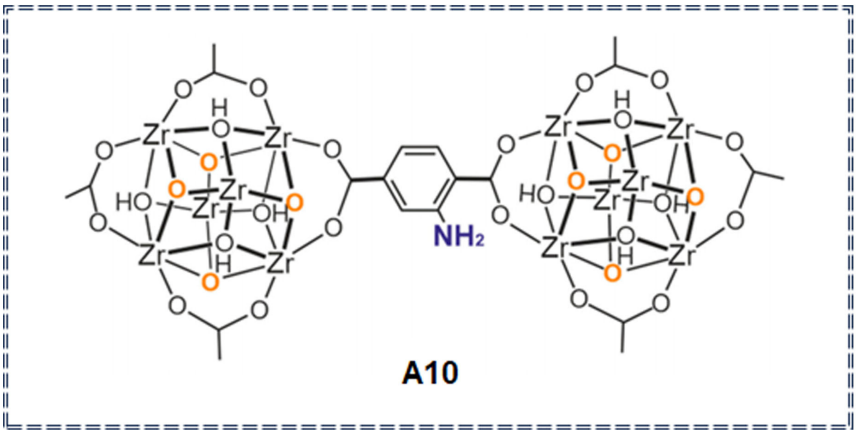

Figure 10. Structure of compound A10. (Reproduced with permission from ref. [90]. copyright 2023 Multidisciplinary Digital Publishing Institute).

Li et al. synthesized a luminescent MOF (LMOF) in situ using 2,2,6,6-tetramethyl-1-piperidinyloxy (TEMPO)-oxidized cellulose nanofibers (TOCNF) as a template, creating TOCNF/LMOF hybrids (A11) that were fabricated into two-dimensional hybridization pads for detecting methyl-parathion (Figure 11a,b) [77,91]. The ligand 1,2,4,5-tetrakis (4-carboxyphenyl) benzene (H4TCPB) within the LMOF exhibits AIE properties (Figure 11c), which enhance fluorescence by restricting the rotation and vibration of the phenyl ring and inhibiting nonradiative decay pathways. This enhancement improves the interaction between the ligand and the target analyte, thus boosting the sensing capability. The detection of methyl-parathion with A11 relies on the interaction between the ligand and the pesticide, leading to fluorescence quenching through charge transfer (Figure 11d,e). This approach enables quantitative detection of pesticides through changes in fluorescence intensity and offers a practical and sustainable platform for AIEgens-based pesticide sensing using MOFs.

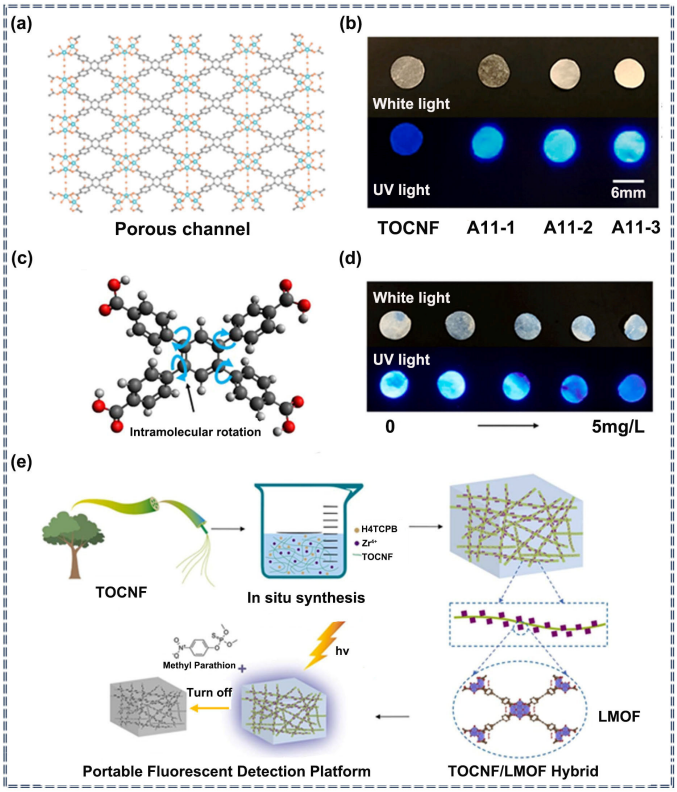

Figure 11. (**a**) Illustration of the porous channel of the LMOF; (**b**) Visual appearance of TOCNF and A11, including three hybrid pads (A11-1, A11-2, and A11-3) under white and UV light; (**c**) Molecular structure of the H4TCPB ligand; (**d**) Illustration of quenching and photographs showing A11 responses at concentrations of 0, 0.2, 1, 2, and 5 mg/L under white and UV light; (**e**) Schematic representation of the sensing mechanism for methyl parathion using A11. (Reproduced with permission from ref. [77]. copyright 2024 Elsevier).

Zhang et al. developed a highly luminescent nanocomposite, GSH-AuNCs@ZIF-8 (A12), by embedding glutathione-protected gold nanoclusters (GSH-AuNCs) within a MOF (ZIF-8) (Figure 12a) [78]. A12 demonstrates sensitive detection capabilities for Cu^{2+} and OPs. The confinement effect of ZIF-8 enhances the stability of GSH-Au NCs and amplifies the AIE effect by restricting their intramolecular motion, significantly improving fluorescence performance. The detection mechanism involves a fluorescence quenching upon binding of A12 to Cu^{2+}. However, TCh can coordinate with Cu^{2+} through sulfhydryl groups, restoring the fluorescence in the Cu^{2+} + A12 system. OPs inhibit AChE activity, reducing TCh production and preventing fluorescence recovery, which allows for the detection of OPs (Figure 12b). As shown in Figure 12c, there is a strong linear relationship

between the green/red fluorescence ratio and the concentrations of Cu^{2+} and glyphosate in the range of 0–5 μM, with detection limits estimated at 0.05 μM for copper ions and 0.93 nM for glyphosate, based on 3σ/k calculations. This sensor enables both semi-quantitative detection by the naked eye and quantitative/accurate detection via a smartphone platform, underscoring its potential for pollution monitoring.

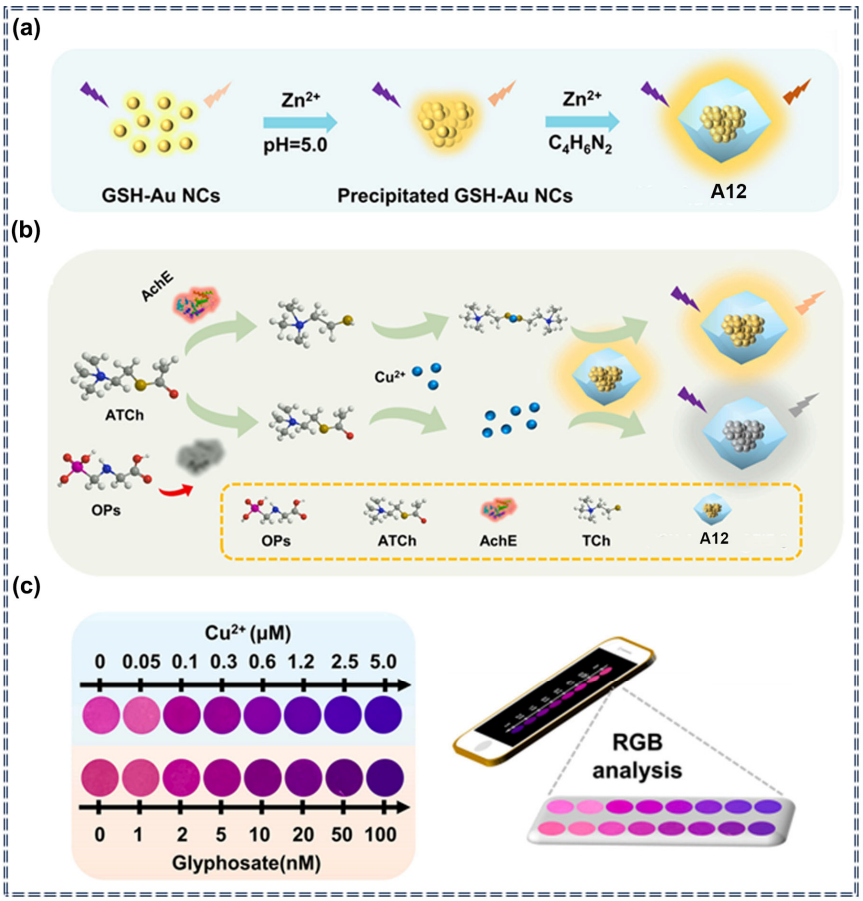

Figure 12. (**a**) Schematic diagram of the synthesis of A12; (**b**) Schematic representation of OP detection based on the Cu^{2+} +A12 system; (**c**) Fluorescence images demonstrating detection with hydrogel A12 upon the addition of different concentrations of Cu^{2+} (0–5 μM) and glyphosate (0–100 nM) under 300 nm UV light; RGB analysis of the fluorescent images was performed using a color recognizer app on a smartphone. (Reproduced with permission from ref. [78]. copyright 2023 Elsevier).

The aforementioned studies leverage the unique properties of AIEgens and MOF materials (such as UiO-66-NH_2 and GSH-Au NCs@ZIF-8). By employing various mechanisms (including fluorescence enhancement, AIE, metal-ion adsorption, and fluorescence quenching), they achieve highly sensitive and selective detection of pesticides. Some research has focused on developing portable detection platforms (like 2D sensing pads and hydrogel sensors based on smartphone technology) or validating practical applications, thereby highlighting the significant application potential of these composite materials.

3.4. Detection of Pesticides by Supramolecular Assemblies Based on AIEgens

Supramolecular assemblies of AIEgens offer advantages for pesticide detection, including high sensitivity, strong specificity, rapid response, and simple operation [92]. These sensors primarily detect pesticides based on the interaction between supramolecular assemblies of AIEgens and pesticide molecules. When pesticide molecules interact with these assemblies, they specifically bind to the AIEgens, causing a change in fluorescence signal. This fluorescence change can be used to detect the presence and concentration of pesticides.

For example, Guo et al. designed and synthesized an esterase-activated AIE and ESIPT probe (A13), suitable for the sensitive ratio detection of carbaryl (Figure 13a) [79]. This probe functions as a supramolecular system where kaempferol tetraacetate interacts with esterase, resulting in fluorescence changes through supramolecular interactions. The acetate group in A13 acts as the esterase reaction site and initiates AIE + ESIPT. Esterase specifically hydrolyzes A13 into kaempferol, which exhibits AIE + ESIPT properties. Carbaryl inhibits esterase activity, reducing the generation of kaempferol, and thus enabling the ratio detection of carbaryl by measuring the fluorescence emission decrease at 415 nm and the ESIPT emission increase at 530 nm (Figure 13b,c). A13 has also been successfully used in real sample detection, presenting a new approach for constructing robust pesticide detection systems.

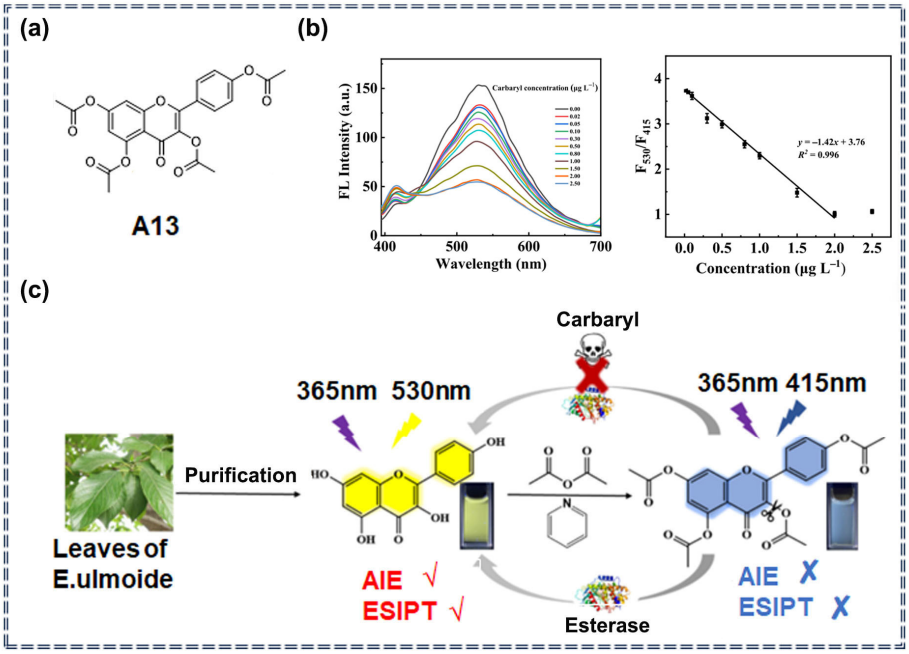

Figure 13. (**a**) Structure of compound A13; (**b**) Fluorescence spectra of kaempferol tetraacetate (10.00 μg mL^{-1}) incubated with esterase (0.60 U mL^{-1}) in the presence of carbaryl (0–2.50 μg L^{-1}) at pH 7.4, showing the linear relationship between F_{530}/F_{415} and the concentration of carbaryl; (**c**) Schematic representation of the activatable AIE + ESIPT probe for ratiometric sensing of carbaryl. (Reproduced with permission from ref. [79]. copyright 2022 Elsevier).

Wu et al. developed a novel supramolecular AIE fluorescent probe, LIQ-TPA-TZ@HSA (A14), for real-time detection of fipronil (FPN) (Figure 14a) [80]. A14 is created by embedding the AIE-active fluorescent compound LIQ-TPA-TZ into the binding pocket of serum albumin (HSA). Upon exposure to FPN, LIQ-TPA-TZ is released into the solution, causing fluorescence changes that facilitate detection. The AIE and intramolecular charge transfer properties of LIQ-TPA-TZ enhance the sensitivity of A14, enabling effective colorimetric analysis of FPN. Additionally, A14 can be applied to portable paper test strips for quick and convenient colorimetric determination of FPN by visual inspection (Figure 14b), offering a practical platform for pesticide detection using supramolecular fluorescent probes.

Yuan et al. designed and synthesized a tetraphenyl ethylene derivative, TPE-4P (A15), functionalized with four pillar[5]arenes as a fluorescent chemical sensor for paraquat detection (Figure 15a) [81]. The pillar[5]arenes in A15 serve as recognition units for capturing paraquat molecules. When paraquat forms a host-guest complex with the pillar[5]arenes, the energy of the excited TPE molecules is dissipated as light radiation, resulting in strong fluorescence emission and allowing for the quantitative detection of paraquat. Additionally, the A15 solution was used to create a test paper that simplifies paraquat detection, demonstrating the excellent potential for practical applications (Figure 15b). The successful

performance of A15 in paraquat detection offers a new perspective on the development of pesticide sensors and shows significant potential for future growth.

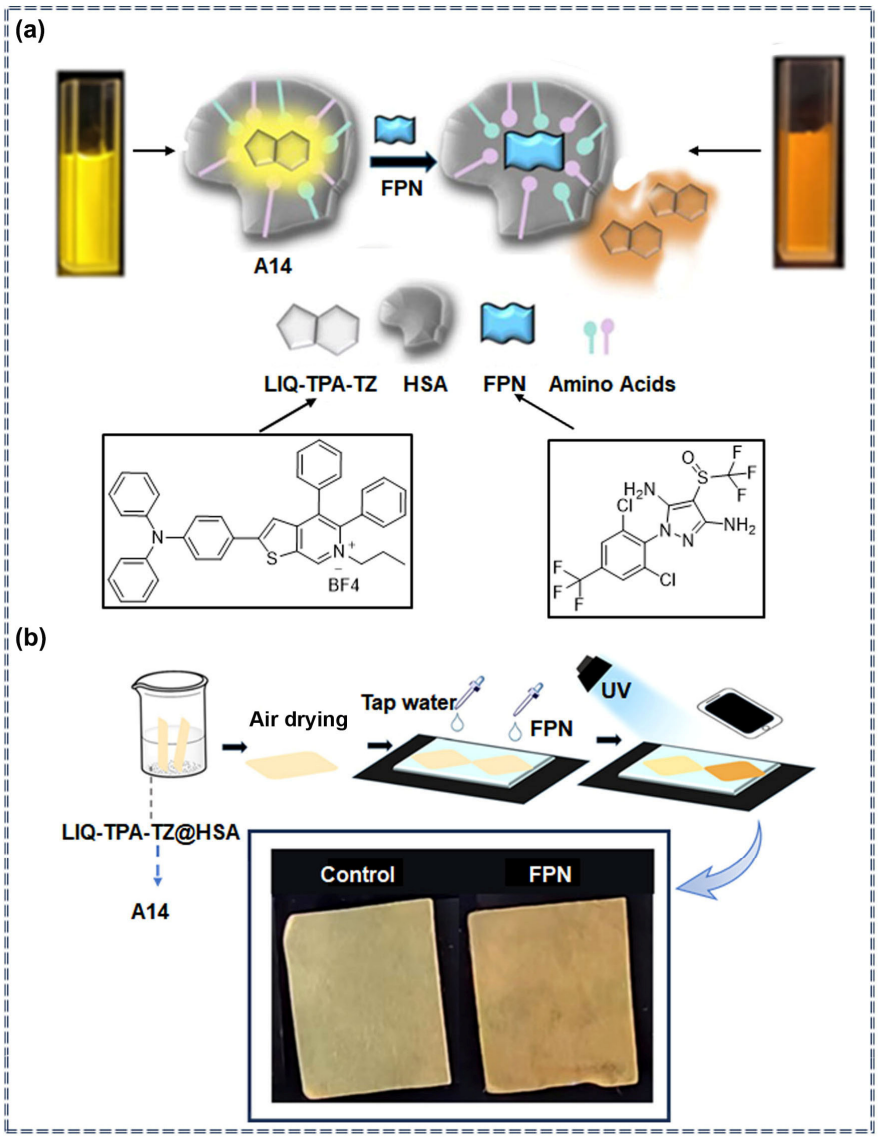

Figure 14. (**a**) Schematic illustration of the A14 probe for the colorimetric and ratiometric detection of FPN (Inset: Structures of LIQ-TPA-TZ and FPN); (**b**) Preparation and testing procedures of the A14-based paper strips; inset: Photographs of the A14-based paper strip in the absence (left) and presence (right) of FPN under a UV lamp (365 nm). (Reproduced with permission from ref. [80]. copyright 2023 Royal Society Chemistry Publishing).

Singh et al. developed a simple and rapid fluorescent probe based on an anionic TPE derivative Su-TPE (A16) for detecting trypsin and methyl paraoxon (Figure 16) [82]. This probe operates through a supramolecular assembly formed between A16 and a polycationic protamine molecule (PrS). A16 does not fluoresce in isolation but emits intense fluorescence when aggregated. PrS, a cationic polyelectrolyte and natural substrate for trypsin, electrostatically interacts with the tetra-anionic A16 molecules, causing their aggregation and the formation of supramolecular complexes (A16/PrS). In the presence of trypsin, PrS is enzymatically degraded, leading to the disintegration of the supramolecular assembly and enabling trypsin detection. When methyl paraoxon (POM) is present, trypsin activity is inhibited, and the fluorescence of the A16/PrS system is restored, allowing for the detection of OPs. This probe, with a detection limit of 500 μM for POM, offers

a simple and convenient method for detecting OPs and shows significant potential for practical applications.

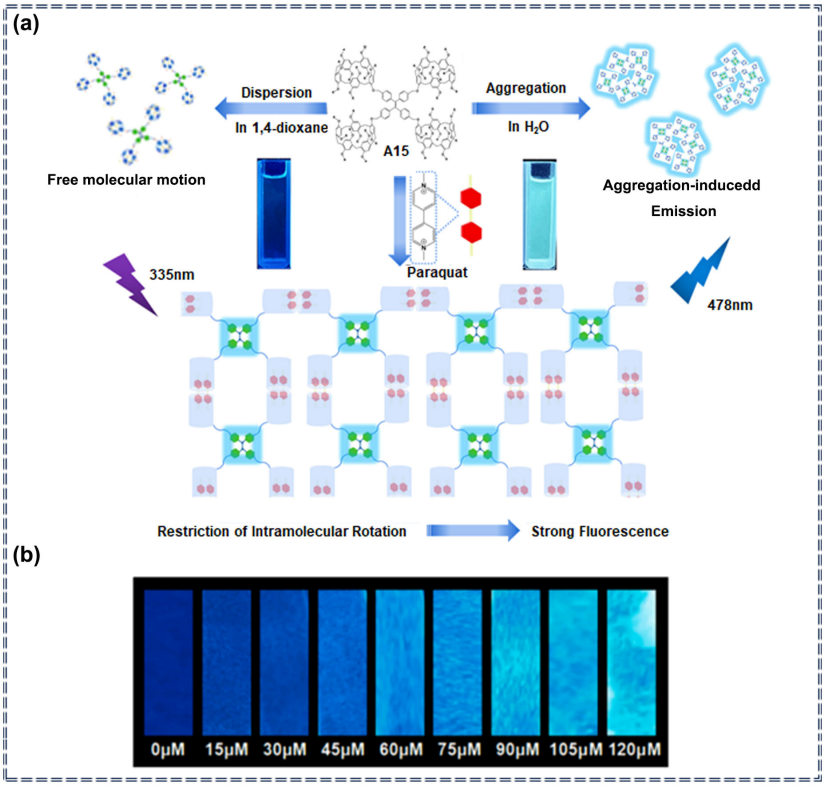

Figure 15. (**a**) Schematic structure of the compound A15 and illustration of the paraquat sensing process; (**b**) Fluorescence intensity changes of A15-based test strips after treatment with varying concentrations of paraquat (0–120 μM). (Reproduced with permission from ref. [81]. copyright 2022 Elsevier).

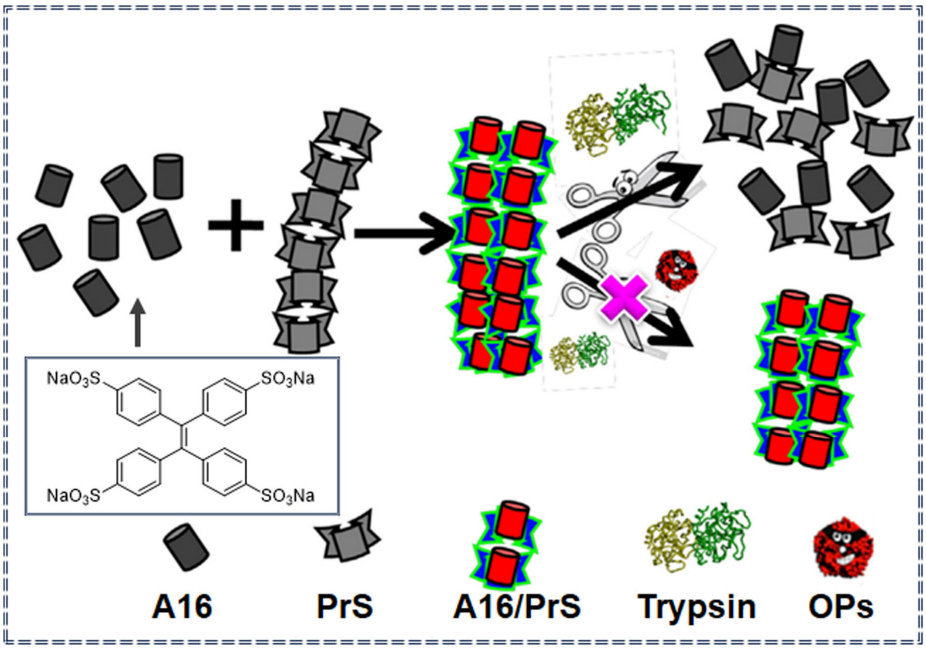

Figure 16. Schematic representation of PrS-dependent AIE of A16 and its application for the detection of trypsin and OPs. Inset: Chemical structure of A16 (Reproduced with permission from ref. [82]. copyright 2021 Elsevier).

The studies utilize materials with AIE properties and supramolecular characteristics (e.g., kaempferol tetraacetate, LIQ-TPA-TZ@HSA, TPE-4P, and Su-TPE/PrS) to design fluorescent sensors. By employing mechanisms like the AIE principle and host-guest interactions, they achieve sensitive and selective detection of pesticides and biological enzymes. Portable detection platforms, such as test strips, have been developed, emphasizing the potential for co-developing supramolecular and AIE materials.

3.5. Detection of Pesticides by Porous Organic Polymer Sensors Based on AIEgens

Integrating AIEgens with porous organic polymers boosts sensitivity, selectivity, multifunctionality, stability, and reusability in pesticide detection. This approach utilizes the combined effects of AIE and various mechanisms to achieve effective sensing and detection.

For example, in 2020, Wang et al. synthesized three fluorescent porous organic polymers containing N-benzylcarbazole groups PAN-C (A17-1), PAN-C-Br (A17-2), and PAN-C-OCH_3 (A17-3) through a one-step polymerization reaction for the identification and detection of six pesticides in water (Figure 17a,b) [83]. The carbazole moiety in these polymers is electron-rich due to the conjugation between the benzene ring and the nitrogen atom, while the pesticides are electron-deficient due to the presence of electron-withdrawing groups such as phosphorothioates, nitro groups, and electronegative fluorine and chlorine atoms. This results in a higher LUMO energy for the polymers compared to the pesticides, allowing for excited-state electron transfer from the LUMO orbitals of the polymer to the pesticide molecules, which leads to fluorescence quenching. Additionally, A17-1-coated sensing test strips were used for pesticide detection, demonstrating a rapid color change within 1–2 s upon contact with the pesticide solution, indicating a fast fluorescent response (Figure 17c). The paper could be easily regenerated by rinsing with ethanol, with the bright cyan color and fluorescence intensity remaining stable after 12 cycles, showcasing excellent reusability (Figure 17d).

Inspired by the above-mentioned work, in 2022, Wang et al. synthesized two micro/mesoporous fluorescent polymers, JY1 (denoted as A18-1) and JY2 (denoted as A18-2), which feature AIE-active chromophores for visual detection of pesticides (Figure 18a) [84]. These probes are capable of detecting four pesticides: imidacloprid (IDP), triflumizole (TFZ), lambda-cyhalothrin (LCT), and cyfluthrin (CFT). The detection mechanism relies on a donor-excited PET process. Under UV light, electrons in the ground state of the chromophore are excited to the LUMO orbitals. In this excited state, the electrons can transfer to the LUMO orbitals of the pesticide molecules, leading to fluorescence quenching (Figure 18b). By introducing AIEgens into porous fluorescent polymers, the high sensitivity and anti-interference ability for pesticide detection could be achieved. Moreover, A18-1 has been developed into a portable fluorescent detection plate, enabling convenient and reusable on-site monitoring and early warning of pesticide residues (Figure 18c). This advancement offers significant potential for practical applications in pesticide detection.

In the same year, Wang et al. also synthesized two AIE-active fluorescent porous polymers, PAN-TPE-1 (A19-1) and PAN-TPE-2 (A19-2) (Figure 19a,b), and investigated their chemical sensing properties for five pesticides: IDP, acetamiprid (AMP), TFZ, indoxacarb (IXC), and LCT [85]. They evaluated the fluorescence spectra of A19-1 and A19-2 in aqueous solutions with varying pesticide concentrations and quantitatively assessed their sensitivity using the fluorescence quenching Stern–Volmer coefficient (K_{SV}) and LOD. They also conducted interference experiments to test the ability of the polymers to detect pesticides in complex environments. A19-1 exhibited impressive K_{SV} and LOD values of 53,745 M^{-1} and 28 ppb for IDP, respectively, which are significantly higher than those reported for other porous materials and exceed those for the other four pesticides by factors of 3 to 10 [93]. Additionally, A19-1 and A19-2 were prepared into a fluorescence detection plate for visualization and practical detection experiments, as shown in Figure 19c. This study highlights the strong pesticide recognition ability of these probes and demonstrates the promising potential of AIE-activated porous polymers for pesticide detection.

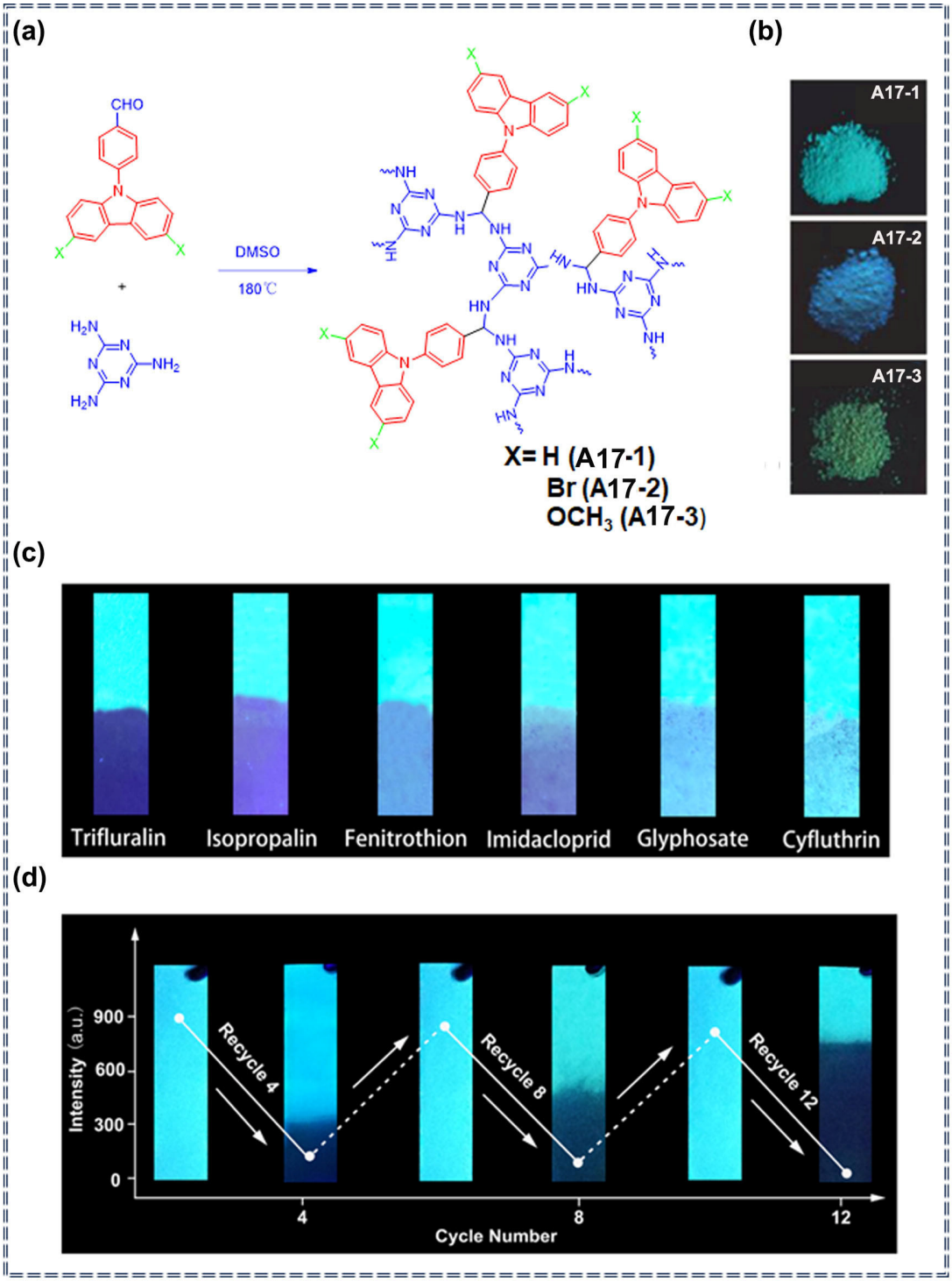

Figure 17. (**a**) Illustration of the synthesis of carbazole-based porous polyaminals; (**b**) Photographs of the solid A17-1, A17-2, and A17-3 under UV light at an excitation wavelength of 365 nm; (**c**) Sensing experiments of A17-1 test paper for six pesticides in water medium at a concentration of 35 μM; (**d**) Recycling sensing experiments of A17-1 for trifluralin in the water medium at a concentration of 58 μM. (Reproduced with permission from ref. [83]. copyright 2020 American Chemical Society).

The above three studies employ fluorescent porous polymers and AIE molecules to create composite luminescent materials. By utilizing their fluorescence characteristics and porous structures, along with mechanisms such as PET or IFE, they enable highly sensitive and selective detection of pesticides.

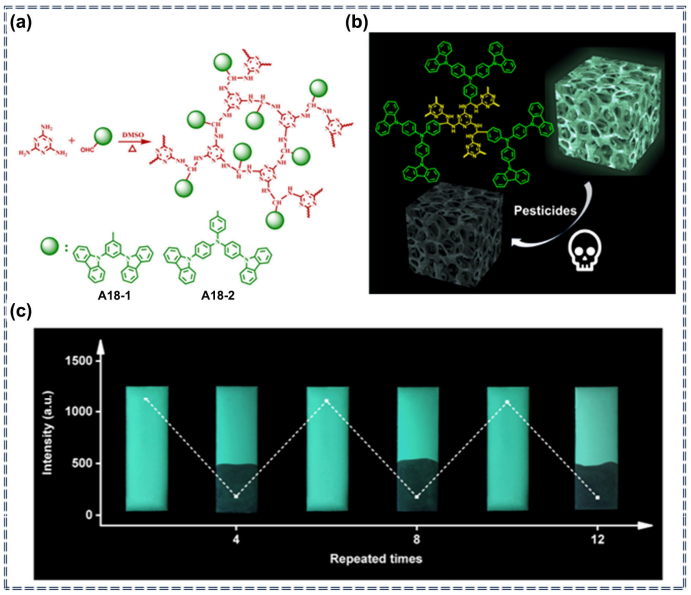

Figure 18. (**a**) Synthesis and structure of the micro-/mesoporous fluorescent polymers A18-1 and A18-2; (**b**) Mechanism of pesticide detection using A18; (**c**) Repeatability of pesticide detection experiments with the A18-1 plate in water at an IDP concentration of 29 μM. (Reproduced with permission from ref. [84]. copyright 2022 American Chemical Society).

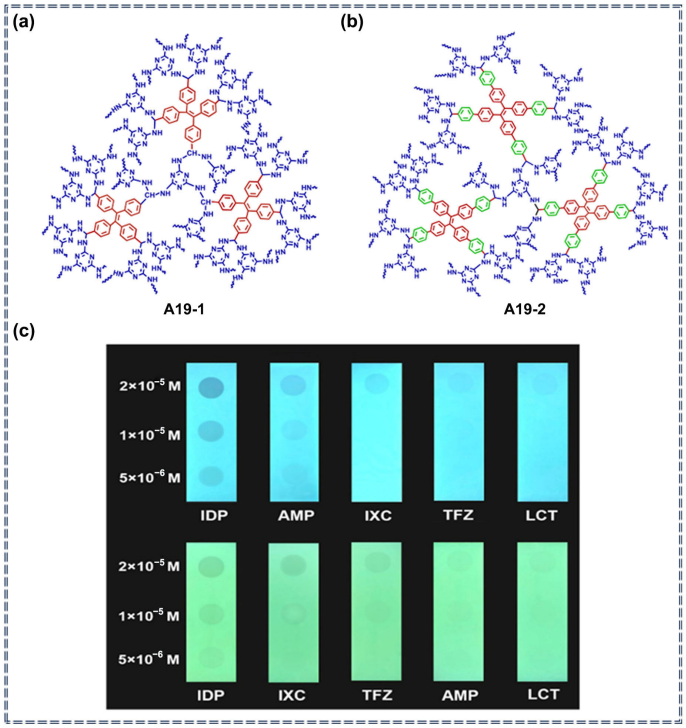

Figure 19. (**a**) Chemical structures of A19-1; (**b**) Chemical structures of A19-2; (**c**) Visual sensing experiments of A19-1 (top) and A19-2 (bottom) fluorescent plates for detecting five pesticides at different concentrations in a water medium. (Reproduced with permission from ref. [85]. copyright 2022 American Chemical Society).

3.6. Detection of Pesticides by Lateral Flow Immunoassay Sensors Based on AIEgens

Lateral flow immunoassay (LFIA) is a rapid and straightforward technology used for detecting small molecules (e.g., pesticides, antibiotics, mycotoxins), foodborne pathogens, allergens, and biological targets (e.g., nucleic acids). The integration of AIEgens with LFIA

can enhance detection sensitivity, reduce autofluorescence interference, improve fluorescence stability, broaden the detection range, and support simple, rapid, and visual detection.

Lai et al. synthesized doped AIE polymer microspheres (DAIEPMs) and 2,3-bis(4-(bis(4-(tert-butyl)phenyl)amino)-phenyl)-fumaronitrile polymer microspheres (BAPFPMs) using a microemulsion method [86]. They electrostatically adsorbed DAIEPMs onto the chlorothalonil (CTN) antibody to form the immune probe DAIEPMs@mAb (A20) (Figure 20a–c). The excellent AIE behavior and large Stokes shift of DAIEPMs in probe A20 enable it to function as a high-performance fluorescent marker in LFIA for the sensitive detection of CTN. In the absence of CTN, A20 is captured by CTN-BSA on the test line (T-line), while excess A20 migrates and is captured by the secondary antibody (sAb) on the control line (C-line). When CTN is present, A20 binds competitively to CTN, preventing its capture by CTN-BSA on the T-line, thus enabling sensitive detection of the organochlorine pesticide chlorothalonil (Figure 20d). The LFIA coupled with AIEgens achieved highly sensitive and specific detection of CTN with a low detection limit of 0.012 ng/mL. This method offers a novel strategy for enhancing the optical properties of fluorescent materials and constructing sensitive and reliable detection platforms.

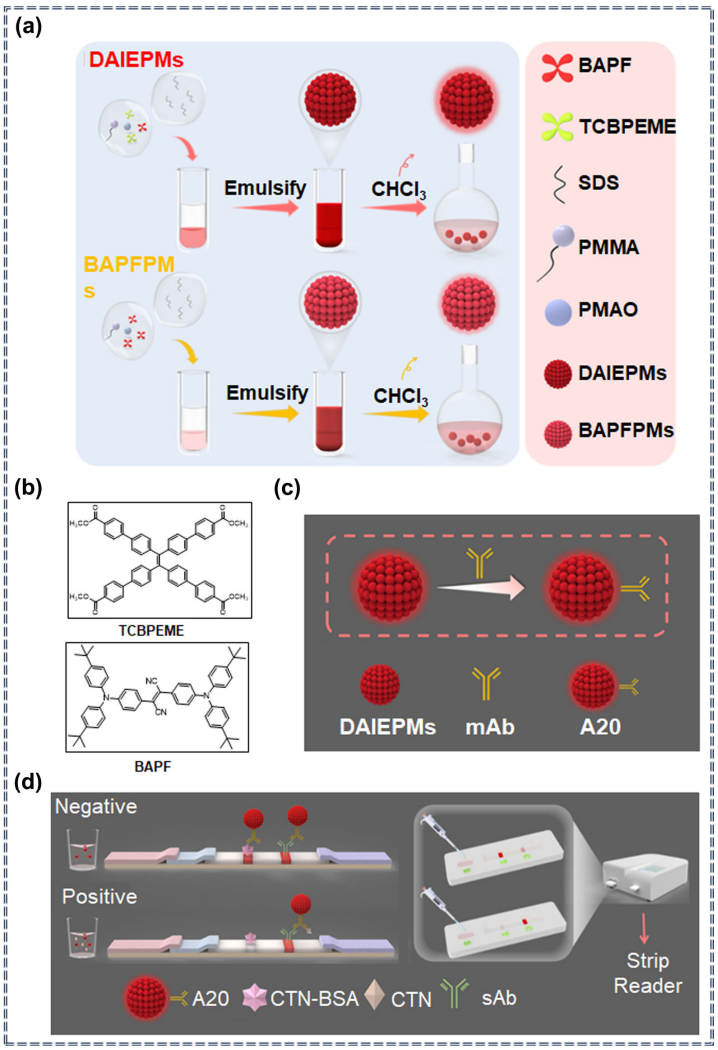

Figure 20. (**a**) Detailed synthesis steps of DAIEPMs and BAPFPMs; (SDS: sodium do-decyl sulfate; PMMA: Poly (methyl methacrylate); PMAO: Poly (maleicanhydride-alt-1-octadecene)); (**b**) Structures of TCBPEME (top) and BAPF (bottom); (**c**) Synthesis steps of A20; (**d**) Sensing performance of A20 for CTN detection and schematic diagram of CTN test strips. (Reproduced with permission from ref. [86]. copyright 2020 American Chemical Society).

The detection methods discussed incorporate AIE characteristics into LFIA techniques, enhancing sensitivity for pesticide detection. In practical applications, these methods demonstrate strong recovery rates and low coefficients of variation, offering a novel approach to improve the optical properties of AIE materials and develop reliable detection platforms.

4. Conclusions

In summary, this review underscores the recent advancements in AIE-based fluorescent sensors for detecting pesticide residues, highlighting their potential to mitigate the environmental challenges associated with agricultural chemicals. The flexibility of AIE-based sensors is demonstrated through their various forms, including organic small-molecule sensors, metal-organic frameworks, metal nanoclusters, supramolecular assemblies, fluorescent porous organic polymers, and lateral flow assays. These sensors offer practical solutions to the limitations of traditional instrumental analyses, providing high sensitivity, specificity, and user-friendly operation.

However, several challenges persist despite these advancements. The complexity involved in AIEgens synthesis often leads to increased costs, which can hinder their practical deployment, particularly for rapid, on-site testing. Environmental factors may introduce interferences that affect sensor performance, and existing sensors may not cover all pesticide types, especially newer or less common ones. Additionally, ensuring the long-term stability and durability of these sensors under varied environmental conditions remains a significant concern.

Addressing these challenges requires continued efforts to enhance material performance, optimize sensor design, and integrate advanced technologies. Advances in these areas will improve the practicality and broader applicability of AIEgens-based sensors, facilitating more effective and reliable pesticide detection in real-world scenarios. Future research and development in this field are crucial for meeting the growing demand for sensitive, accurate, and efficient pesticide monitoring, ultimately contributing to better environmental and public health outcomes.

Author Contributions: Conceptualization, B.Z. and S.R.; methodology, B.Z.; software, B.Z.; validation, B.Z., S.R. and H.L.; formal analysis, J.-R.W.; investigation, B.Z.; resources, B.Z.; data curation, B.Z.; writing—original draft preparation, B.Z.; writing—review and editing, J.-R.W.; visualization, J.-R.W.; supervision, J.-R.W. and H.W.; project administration, J.-R.W. and H.W.; funding acquisition, H.L., J.-R.W. and H.W. All authors have read and agreed to the published version of the manuscript.

Funding: This research was funded by the Science and Technology Development Program of Jilin Province (Grant No. 20220201117GX) and the National Natural Science Foundation of China (Grant No. 52473212, 22201096, 21703015).

Data Availability Statement: Not applicable.

Acknowledgments: J.-R.W. thanks the strong support from Lijun Zhang and Bo Gao.

Conflicts of Interest: The authors declare no conflicts of interest.

References

1. Pundir, C.S.; Chauhan, N. Acetylcholinesterase Inhibition-Based Biosensors for Pesticide Determination: A Review. *Anal. Biochem.* **2012**, *429*, 19–31. [CrossRef] [PubMed]
2. Chen, Y.; Liu, H.; Tian, Y.; Du, Y.; Ma, Y.; Zeng, S.; Gu, C.; Jiang, T.; Zhou, J. In Situ Recyclable Surface-Enhanced Raman Scattering-Based Detection of Multicomponent Pesticide Residues on Fruits and Vegetables by the Flower-like MoS_2@Ag Hybrid Substrate. *ACS Appl. Mater. Interfaces* **2020**, *12*, 14386–14399. [CrossRef] [PubMed]
3. Songa, E.A.; Okonkwo, J.O. Recent Approaches to Improving Selectivity and Sensitivity of Enzyme-Based Biosensors for Organophosphorus Pesticides: A Review. *Talanta* **2016**, *155*, 289–304. [CrossRef] [PubMed]
4. Wang, J. Fluorescent Peptide Probes for Organophosphorus Pesticides Detection. *J. Hazard. Mater.* **2020**, *389*, 122074. [CrossRef]
5. Carvalho, F.P. Pesticides, Environment, and Food Safety. *Food Energy Secur.* **2017**, *6*, 48–60. [CrossRef]
6. Singh, R. Progress and Challenges in the Detection of Residual Pesticides Using Nanotechnology Based Colorimetric Techniques. *Trends Environ. Anal. Chem.* **2020**, *26*, e00086. [CrossRef]

7. Haraux, E.; Tourneux, P.; Kouakam, C.; Stephan-Blanchard, E.; Boudailliez, B.; Leke, A.; Klein, C.; Chardon, K. Isolated Hypospadias: The Impact of Prenatal Exposure to Pesticides, as Determined by Meconium Analysis. *Environ. Int.* **2018**, *119*, 20–25. [CrossRef]
8. Lu, Y.; Wei, M.; Wang, C.; Wei, W.; Liu, Y. Enhancing Hydrogel-Based Long-Lasting Chemiluminescence by a Platinum-Metal Organic Framework and its Application in Array Detection of Pesticides and D-Amino Acids. *Nanoscale* **2020**, *12*, 4959–4967. [CrossRef]
9. Zhou, P.; Han, K. ESIPT-Based AIE Luminogens: Design Strategies, Applications, and Mechanisms. *Aggregate* **2022**, *3*, e160. [CrossRef]
10. Zhou, B.; Li, X. The Monitoring of Chemical Pesticides Pollution on Ecological Environment by GIS. *Environ. Technol. Innov.* **2021**, *23*, 101506. [CrossRef]
11. Tang, F.H.M.; Lenzen, M.; McBratney, A.; Maggi, F. Risk of Pesticide Pollution at the Global Scale. *Nat. Geosci.* **2021**, *14*, 206–210. [CrossRef]
12. Liu, M.; Wei, J.; Wang, Y.; Ouyang, H.; Fu, Z. Dopamine-Functionalized Upconversion Nanoparticles as Fluorescent Sensors T for Organophosphorus Pesticide Analysis. *Talanta* **2019**, *195*, 706–712. [CrossRef]
13. Ishaq, Z.; Nawaz, M.A. Analysis of Contaminated Milk with Organochlorine Pesticide Residues Using Gas Chromatography. *Int. J. Food Prop.* **2018**, *21*, 879–891. [CrossRef]
14. Tazarv, M.; Faraji, H.; Moghimi, A.; Azizinejad, F. Bursting-bubble Flow Microextraction Combined with Gas Chromatography to Analyze Organophosphorus Pesticides in Aqueous Samples. *J. Sep. Sci.* **2021**, *44*, 2965–2971. [CrossRef]
15. Dane, A.J.; Havey, C.D.; Voorhees, K.J. The Detection of Nitro Pesticides in Mainstream and Sidestream Cigarette Smoke Using Electron Monochromator-Mass Spectrometry. *Anal. Chem.* **2006**, *78*, 3227–3233. [CrossRef]
16. Tabibi, A.; Jafari, M.T. High Efficient Solid-Phase Microextraction Based on a Covalent Organic Framework for Determination of Trifluralin and Chlorpyrifos in Water and Food Samples by GC-CD-IMS. *Food Chem.* **2022**, *373*, 131527. [CrossRef] [PubMed]
17. Zhang, H.; Chen, Z.; Yang, G.; Wang, W.; Li, X.; Li, R.; Wu, Y. Microwave Pretreatment and Gas Chromatography–Mass Spectrometry Determination of Herbicide Residues in Onion. *Food Chem.* **2008**, *108*, 322–328. [CrossRef]
18. Hassan, J.; Farahani, A.; Shamsipur, M.; Damerchili, F. Rapid and Simple Low Density Miniaturized Homogeneous Liquid–Liquid Extraction and Gas Chromatography/Mass Spectrometric Determination of Pesticide Residues in Sediment. *J. Hazard. Mater.* **2010**, *184*, 869–871. [CrossRef]
19. Bruzzoniti, M.C.; Sarzanini, C.; Costantino, G.; Fungi, M. Determination of Herbicides by Solid Phase Extraction Gas Chromatography–Mass Spectrometry in Drinking Waters. *Anal. Chim. Acta* **2006**, *578*, 241–249. [CrossRef]
20. Notardonato, I.; Salimei, E.; Russo, M.V.; Avino, P. Simultaneous Determination of Organophosphorus Pesticides and Phthalates in Baby Food Samples by Ultrasound–Vortex-Assisted Liquid–Liquid Microextraction and GC–IT/MS. *Anal. Bioanal. Chem.* **2018**, *410*, 3285–3296. [CrossRef]
21. Wang, H.; Qu, B.; Liu, H.; Ding, J.; Ren, N. Analysis of Organochlorine Pesticides in Surface Water of the Songhua River Using Magnetoliposomes as Adsorbents Coupled with GC-MS/MS Detection. *Sci. Total Environ.* **2018**, *618*, 70–79. [CrossRef] [PubMed]
22. Harshit, D.; Charmy, K.; Nrupesh, P. Organophosphorus Pesticides Determination by Novel HPLC and Spectrophotometric Method. *Food Chem.* **2017**, *230*, 448–453. [CrossRef] [PubMed]
23. Liu, W.; Quan, J.; Hu, Z. Detection of Organophosphorus Pesticides in Wheat by Ionic Liquid-Based Dispersive Liquid-Liquid Microextraction Combined with HPLC. *J. Anal. Methods Chem.* **2018**, *2018*, 8916393. [CrossRef]
24. Simpson, A.J.; Simpson, M.J.; Soong, R. Environmental Nuclear Magnetic Resonance Spectroscopy: An Overview and a Primer. *Anal. Chem.* **2018**, *90*, 628–639. [CrossRef]
25. Xu, N.; Ding, Y.; Ai, H.; Fei, J. Acetylene Black-Ionic Liquids Composite Electrode: A Novel Platform for Electrochemical Sensing. *Microchim. Acta* **2010**, *170*, 165–170. [CrossRef]
26. Gajdár, J.; Barek, J.; Fischer, J. Antimony Film Electrodes for Voltammetric Determination of Pesticide Trifluralin. *J. Electroanal. Chem.* **2016**, *778*, 1–6. [CrossRef]
27. Cai, Y.; Fang, J.; Wang, B.; Zhang, F.; Shao, G.; Liu, Y. A Signal-on Detection of Organophosphorus Pesticides by Fluorescent Probe Based on Aggregation-Induced Emission. *Sens. Actuators B Chem.* **2019**, *292*, 156–163. [CrossRef]
28. Zhou, B.; Jiang, Q.; Li, J.; Yan, S.; Shen, J.; Liu, L.; Yin, M. An AIE Star Polymer with Enhanced Co-Delivery of Drug and Gene for Synergistic Pest Control. *Chin. J. Chem.* **2023**, *41*, 2671–2678. [CrossRef]
29. Patel, D.A.; Anand, T.; Jali, B.R.; Sahoo, S.K. 4,4′-Sulfonyldianiline Derived AIE Luminogen for the Detection of Ofloxacin. *ChemPlusChem* **2024**. [CrossRef]
30. Xu, T.; Fu, Q.; Qingru, Z.; Wang, Z.; Liu, X.; Xiao, S.; Jiang, X.; Lu, Y.; Gong, Z.; Wu, Y.; et al. A Simple Fluorescence Pyrocatechol–Polyethyleneimine Detection Method for 3-MCPD. *Anal. Methods* **2024**, *16*, 276–283. [CrossRef]
31. Xue, J.; Mao, K.; Cao, H.; Feng, R.; Chen, Z.; Du, W.; Zhang, H. Portable Sensors Equipped with Smartphones for Organophosphorus Pesticides Detection. *Food Chem.* **2024**, *434*, 137456. [CrossRef] [PubMed]
32. Chua, M.H.; Hui, B.Y.K.; Chin, K.L.O.; Zhu, Q.; Liu, X.; Xu, J. Recent Advances in Aggregation-Induced Emission (AIE)-Based Chemosensors for the Detection of Organic Small Molecules. *Mater. Chem. Front.* **2023**, *7*, 5561–5660. [CrossRef]
33. Adarsh, N.; Krishnan, M.S.; Ramaiah, D. Sensitive Naked Eye Detection of Hydrogen Sulfide and Nitric Oxide by Aza-BODIPY Dyes in Aqueous Medium. *Anal. Chem.* **2014**, *86*, 9335–9342. [CrossRef] [PubMed]

34. Chen, X.X.; Niu, L.Y.; Shao, N.; Yang, Q.Z. BODIPY-Based Fluorescent Probe for Dual-Channel Detection of Nitric Oxide and Glutathione: Visualization of Cross-Talk in Living Cells. *Anal. Chem.* **2019**, *91*, 4301–4306. [CrossRef] [PubMed]
35. Kwon, N. Metal-Coordinated Fluorescent and Luminescent Probes for Reactive Oxygen Species (ROS) and Reactive Nitrogen Species (RNS). *Coord. Chem. Rev.* **2021**, *427*, 213581. [CrossRef]
36. Peng, H.; Cheng, Y.; Dai, C.; King, A.L.; Predmore, B.L.; Lefer, D.J.; Wang, B. A Fluorescent Probe for Fast and Quantitative Detection of Hydrogen Sulfide in Blood. *Angew. Chem. Int. Ed.* **2011**, *50*, 9672–9675. [CrossRef]
37. Kumar, N. Recent Developments of Fluorescent Probes for the Detection of Gasotransmitters (NO, CO and H_2S). *Coord. Chem. Rev.* **2013**, *257*, 2335–2347. [CrossRef]
38. Hammers, M.D.; Taormina, M.J.; Cerda, M.M.; Montoya, L.A.; Seidenkranz, D.T.; Parthasarathy, R.; Pluth, M.D. A Bright Fluorescent Probe for H_2S Enables Analyte-Responsive, 3D Imaging in Live Zebrafish Using Light Sheet Fluorescence Microscopy. *J. Am. Chem. Soc.* **2015**, *137*, 10216–11022. [CrossRef]
39. Yang, J.; Chen, S.W.; Zhang, B.; Tu, Q.; Wang, J.; Yuan, M.-S. Non-Biological Fluorescent Chemosensors for Pesticides Detection. *Talanta* **2022**, *240*, 123200. [CrossRef]
40. Luo, J.; Xie, Z.; Lam, J.W.Y.; Cheng, L.; Tang, B.Z.; Chen, H.; Qiu, C.; Kwok, H.S.; Zhan, X.; Liu, Y.; et al. Aggregation-Induced Emission of 1-Methyl-1,2,3,4,5-Pentaphenylsilole. *Chem. Commun.* **2001**, *18*, 1740–1741. [CrossRef]
41. Cai, X.; Liu, B. Aggregation-Induced Emission: Recent Advances in Materials and Biomedical Applications. *Angew. Chem. Int. Ed.* **2020**, *59*, 9868–9886. [CrossRef] [PubMed]
42. Mei, J.; Leung, N.L.C.; Kwok, R.T.K.; Lam, J.W.Y.; Tang, B.Z. Aggregation-Induced Emission: Together We Shine, United We Soar! *Chem. Rev.* **2015**, *115*, 11718–11940. [CrossRef] [PubMed]
43. Zhou, C.; Ma, J.; Sun, D.W. Grouping Illuminants by Aggregation-Induced Emission (AIE) Mechanisms for Designing Sensing Platforms for Food Quality and Safety Inspection. *Trends Food Sci. Technol.* **2023**, *134*, 232–246. [CrossRef]
44. Deng, X.; Xu, Z.; Zhang, Z.; Zhang, W.; Li, J.; Zheng, L.; Chen, X.; Pan, Y.; Qiu, P.; Wang, D.; et al. In Vivo 3-Photon Fluorescence Imaging of Mouse Subcortical Vasculature Labeled by AIEgen Before and After Craniotomy. *Adv. Funct. Mater.* **2022**, *32*, 2205151. [CrossRef]
45. Wang, J.; Liu, X.; Wang, J.; Li, F.; Jiang, H.; Liu, L. Recent Progress on the Construction and Application of Dithienylethene-Based Photochromic AIEgens. *Luminescence* **2023**, *39*, e4546. [CrossRef]
46. Barman, D.; Narang, K.; Parui, R.; Zehra, N.; Khatun, M.N.; Adil, L.R.; Iyer, P.K. Review on Recent Trends and Prospects in π-Conjugated Luminescent Aggregates for Biomedical Applications. *Aggregate* **2022**, *3*, e172. [CrossRef]
47. Chen, P.; Lv, P.; Guo, C.-S.; Wang, R.P.; Su, X.; Feng, H.T.; Tang, B.Z. Enantioselective Recognition Based on Aggregation-Induced Emission. *Chin. Chem. Lett.* **2023**, *34*, 108041. [CrossRef]
48. Ye, F.Y.; Hu, M.; Zheng, Y.S. Advances and Challenges of Metal Ions Sensors Based on AIE Effect. *Coord. Chem. Rev.* **2023**, *493*, 215328. [CrossRef]
49. Zhang, Y.; Xie, S.; Zeng, Z.; Tang, B.Z. Functional Scaffolds from AIE Building Blocks. *Matter* **2020**, *3*, 1862–1892. [CrossRef]
50. Würthner, F. Aggregation-Induced Emission (AIE): A Historical Perspective. *Angew. Chem. Int. Ed.* **2020**, *59*, 14192–14196. [CrossRef]
51. Li, Z.; Tang, B.Z.; Wang, D. Bioinspired AIE Nanomedicine: A Burgeoning Technology for Fluorescence Bioimaging and Phototheranostics. *Adv. Mater.* **2024**, *36*, 2406047. [CrossRef] [PubMed]
52. Gao, A.; Wang, Q.; Wu, H.; Zhao, J.W.; Cao, X. Research Progress on AIE Cyanostilbene-Based Self-Assembly Gels: Design, Regulation and Applications. *Coord. Chem. Rev.* **2022**, *471*, 214753. [CrossRef]
53. Wang, H.; Li, Q.; Alam, P.; Bai, H.; Bhalla, V.; Bryce, M.R.; Cao, M.; Chen, C.; Chen, S.; Chen, X.; et al. Aggregation-Induced Emission (AIE), Life and Health. *ACS Nano* **2023**, *17*, 14347–14405. [CrossRef]
54. Lee, K.W.; Chen, H.; Wan, Y.; Zhang, Z.; Huang, Z.; Li, S.; Lee, C.-S. Innovative Probes with Aggregation-Induced Emission Characteristics for Sensing Gaseous Signaling Molecules. *Biomaterials* **2022**, *289*, 121753. [CrossRef] [PubMed]
55. Tong, H.; Hong, Y.; Dong, Y.; Häußler, M.; Lam, J.W.Y.; Li, Z.; Guo, Z.; Guo, Z.; Tang, B.Z. Fluorescent "Light-up" Bioprobes Based on Tetraphenylethylene Derivatives with Aggregation-Induced Emission Characteristics. *Chem. Commun.* **2006**, 3705–3707. [CrossRef]
56. Chen, J.; Law, C.C.W.; Lam, J.W.Y.; Dong, Y.; Lo, S.M.F.; Williams, I.D.; Zhu, D.; Tang, B.Z. Synthesis, Light Emission, Nanoaggregation, and Restricted Intramolecular Rotation of 1,1-Substituted 2,3,4,5-Tetraphenylsiloles. *Chem. Mater.* **2003**, *15*, 1535–1546. [CrossRef]
57. Qin, A.; Lam, J.W.Y.; Tang, B.Z. Luminogenic Polymers with Aggregation-Induced Emission Characteristics. *Prog. Polym. Sci.* **2012**, *37*, 182–209. [CrossRef]
58. Li, X.; Li, M.; Yang, M.; Xiao, H.; Wang, L.; Chen, Z.; Liu, S.; Li, J.; Li, S.; James, T.D. "Irregular" Aggregation-Induced Emission Luminogens. *Coord. Chem. Rev.* **2020**, *418*, 213358. [CrossRef]
59. Gu, Y.; Zhao, Z.; Su, H.; Zhang, P.; Liu, J.; Niu, G.; Li, S.; Wang, Z.; Kwok, R.T.K.; Ni, X.-L.; et al. Exploration of Biocompatible AIEgens from Natural Resources. *Chem. Sci.* **2018**, *9*, 6497–6502. [CrossRef]
60. Chen, S.; Wang, H.; Hong, Y.; Tang, B.Z. Fabrication of Fluorescent Nanoparticles Based on AIE Luminogens (AIE Dots) and Their Applications in Bioimaging. *Mater. Horiz.* **2016**, *3*, 283–293. [CrossRef]
61. Hu, R.; Kang, Y.; Tang, B.Z. Recent Advances in AIE Polymers. *Polym. J.* **2016**, *48*, 359–370. [CrossRef]

62. He, T.; Wang, H.; Chen, Z.; Liu, S.; Li, J.; Li, S. Natural Quercetin AIEgen Composite Film with Antibacterial and Antioxidant Properties for In Situ Sensing of Al^{3+} Residues in Food, Detecting Food Spoilage, and Extending Food Storage Times. *ACS Appl. Bio Mater.* **2018**, *1*, 636–642. [CrossRef] [PubMed]
63. Paul, S.; Daga, P.; Dey, N. Exploring Various Photochemical Processes in Optical Sensing of Pesticides by Luminescent Nanomaterials: A Concise Discussion on Challenges and Recent Advancements. *ACS Omega* **2023**, *8*, 44395–44423. [CrossRef]
64. Mirres, A.C.d.M.; Silva, B.E.P.d.M.d.; Tessaro, L.; Galvan, D.; Andrade, J.C.d.; Aquino, A.; Joshi, N.; Conte-Junior, C.A. Recent Advances in Nanomaterial-Based Biosensors for Pesticide Detection in Foods. *Biosensors* **2022**, *12*, 572. [CrossRef]
65. Naghibi, S.; Chen, T.; Jamshidi Ghahfarokhi, A.; Tang, Y. AIEgen-Enhanced Protein Imaging: Probe Design and Sensing Mechanisms. *Aggregate* **2021**, *2*, e41. [CrossRef]
66. Niu, H.; Ye, T.; Yao, L.; Lin, Y.; Chen, K.; Zeng, Y.; Li, L.; Guo, L.; Wang, J. A Novel Red-to-near-Infrared AIE Fluorescent Probe for Detection of Hg^{2+} with Large Stokes Shift in Plant and Living Cells. *J. Hazard. Mater.* **2024**, *475*, 134914. [CrossRef]
67. Asad, M.; Anwar, M.I.; Abbas, A.; Younas, A.; Hussain, S.; Gao, R.; Li, L.K.; Shahid, M.; Khan, S. AIE Based Luminescent Porous Materials as Cutting-Edge Tool for Environmental Monitoring: State of the Art Advances and Perspectives. *Coord. Chem. Rev.* **2022**, *463*, 214539. [CrossRef]
68. Lee, M.M.S.; Yu, E.Y.; Yan, D.; Chau, J.H.C.; Wu, Q.; Lam, J.W.Y.; Ding, D.; Kwok, R.T.K.; Wang, D.; Tang, B.Z. The Role of Structural Hydrophobicity on Cationic Amphiphilic Aggregation-Induced Emission Photosensitizer-Bacterial Interaction and Photodynamic Efficiency. *ACS Nano* **2023**, *17*, 17004–17020. [CrossRef]
69. Dai, J.; Zhao, Y.; Hou, Y.; Zhong, G.; Gao, R.; Wu, J.; Shen, B.; Zhang, X. Detection of Carboxylesterase 1 and Carbamates with a Novel Fluorescent Protein Chromophore Based Probe. *Dyes Pigm.* **2021**, *192*, 109444. [CrossRef]
70. Liu, W.; Zheng, P.; Xia, Y.; Li, F.; Zhang, M. A Simple AIE Probe to Pesticide Trifluralin Residues in Aqueous Phase: Ultra-Fast Response, High Sensitivity, and Quantitative Detection Utilizing a Portable Platform. *Talanta* **2023**, *269*, 125352. [CrossRef]
71. Zhou, N.; Cai, M.; Zheng, S.; Guo, H.; Yang, F. First Organic Fluorescent Sensor for Pesticide Paclobutrazol Based on Tetraphenylimidazole Schiff Base. *Sens. Actuators B Chem.* **2024**, *417*, 136051. [CrossRef]
72. Cai, Y.; Qiu, Z.; Lin, X.; Zeng, W.; Cao, Y.; Liu, W.; Liu, Y. Self-Assembled Nanomaterials Based on Aggregation-Induced Emission of AuNCs: Fluorescence and Colorimetric Dual-Mode Biosensing of Organophosphorus Pesticides. *Sens. Actuators B Chem.* **2020**, *321*, 128481. [CrossRef]
73. Chen, J.; Chen, X.; Huang, Q.; Li, W.; Yu, Q.; Zhu, L.; Zhu, T.; Liu, S.; Chi, Z. Amphiphilic Polymer-Mediated Aggregation-Induced Emission Nanoparticles for Highly Sensitive Organophosphorus Pesticide Biosensing. *ACS Appl. Mater. Interfaces* **2019**, *11*, 32689–32696. [CrossRef] [PubMed]
74. Liu, Y.; Li, Y.; Luo, X.; Luo, P.; Han, Z.; Peng, Q.; Li, K.; Hou, H.; Zang, S.Q. AIE Ligand-Based Silver Clusters Used for Ethion Detection. *Mater. Chem. Front.* **2021**, *5*, 7982–7986. [CrossRef]
75. Wu, X.; Wang, P.; Hou, S.; Wu, P.; Xue, J. Fluorescence Sensor for Facile and Visual Detection of Organophosphorus Pesticides Using AIE Fluorogens-SiO_2-MnO_2 Sandwich Nanocomposites. *Talanta* **2019**, *198*, 8–14. [CrossRef]
76. Xu, Y.; Pu, Y.; Jiang, H.; Huang, Y.; Shen, C.; Cao, J.; Jiang, W. Highly Sensitive Fluorescent Sensing Platform for Imidacloprid and Thiamethoxam by Aggregation-Induced Emission of the Zr(IV) Metal-Organic Framework. *Food Chem.* **2021**, *375*, 131879. [CrossRef]
77. Zhang, K.; Elder, T.; Cheng, Z.; Zhan, K.; Peng, Y.; Li, M. Cellulose Nanofiber-Templated Metal-Organic Frameworks for Fluorescent Detection of Methyl Parathion Pesticides. *J. Environ. Chem. Eng.* **2024**, *12*, 112670. [CrossRef]
78. Wei, D.; Li, M.; Wang, Y.; Zhu, N.; Hu, X.; Zhao, B.; Zhang, Z.; Yin, D. Encapsulating Gold Nanoclusters into Metal–Organic Frameworks to Boost Luminescence for Sensitive Detection of Copper Ions and Organophosphorus Pesticides. *J. Hazard. Mater.* **2022**, *441*, 129890. [CrossRef]
79. Fan, L.; Tong, C.; Cao, Y.; Long, R.; Wei, Q.; Wang, F.; Tong, X.; Shi, S.; Guo, Y. Highly Specific Esterase Activated AIE plus ESIPT Probe for Sensitive Ratiometric Detection of Carbaryl. *Talanta* **2022**, *246*, 123517. [CrossRef]
80. Ge, J.; Wang, L.J.; Pan, X.; Zhang, C.; Wu, M.Y.; Feng, S. Colorimetric and Ratiometric Supramolecular AIE Fluorescent Probe for the On-Site Monitoring of Fipronil. *Analyst* **2023**, *148*, 5395–5401. [CrossRef]
81. Kang, Z.; Yang, J.; Jiang, J.; Zhao, L.; Zhang, Y.; Tu, Q.; Wang, J.; Yuan, M.-S. Pillar[5]Arenes Modified Tetraphenylethylene as Fluorescent Chemosensor for Paraquat Detection. *Sens. Actuators B Chem.* **2022**, *370*, 132436. [CrossRef]
82. Kaur, J.; Malegaonkar, J.N.; Bhosale, S.V.; Singh, P.K. An Anionic Tetraphenyl Ethylene Based Simple and Rapid Fluorescent Probe for Detection of Trypsin and Paraoxon Methyl. *J. Mol. Liq.* **2021**, *333*, 115980. [CrossRef]
83. Zhang, B.; Li, B.; Wang, Z. Creation of Carbazole-Based Fluorescent Porous Polymers for Recognition and Detection of Various Pesticides in Water. *ACS Sens.* **2020**, *5*, 162–170. [CrossRef]
84. Li, W.; Tang, J.; Wang, Z. Micro-/Mesoporous Fluorescent Polymers and Devices for Visual Pesticide Detection with Portability, High Sensitivity, and Ultrafast Response. *ACS Appl. Mater. Interfaces* **2022**, *14*, 5815–5824. [CrossRef]
85. Zhang, J.; Xue, F.; Wang, Z. AIE-Active Fluorescent Porous Polymers for Recognizable Detection of Imidacloprid and Structure–Property Relationship. *Chem. Mater.* **2022**, *34*, 10701–10710. [CrossRef]
86. Wang, Y.; Zhang, G.; Xiao, X.; Shu, X.; Fei, D.; Guang, Y.; Zhou, Y.; Lai, W. High-Performance Fluorescent Microspheres Based on Fluorescence Resonance Energy Transfer Mode for Lateral Flow Immunoassays. *Anal. Chem.* **2023**, *95*, 17860–17867. [CrossRef]
87. Awiaz, G.; Lin, J.; Wu, A. Recent Advances of Au@Ag Core–Shell SERS-based Biosensors. *Exploration* **2023**, *3*, 20220072. [CrossRef]

88. Xia, X.; Shi, B.; Wang, L.; Liu, Y.; Zou, Y.; Zhou, Y.; Chen, Y.; Zheng, M.; Zhu, Y.; Duan, J.; et al. From Mouse to Mouse-ear Cress: Nanomaterials as Vehicles in Plant Biotechnology. *Exploration* **2021**, *1*, 9–20. [CrossRef]
89. Chen, J.; Wang, Y.; Yu, Y.; Wang, J.; Liu, J.; Ihara, H.; Qiu, H. Composite Materials Based on Covalent Organic Frameworks for Multiple Advanced Applications. *Exploration* **2023**, *3*, 20220144. [CrossRef]
90. Timofeev, K.L.; Kulinich, S.A.; Kharlamova, T.S. NH_2-Modified UiO-66: Structural Characteristics and Functional Properties. *Molecules* **2023**, *28*, 3916. [CrossRef]
91. Lammert, M.; Reinsch, H.; Murray, C.A.; Wharmby, M.T.; Terraschke, H.; Stock, N. Synthesis and Structure of Zr (IV)- and Ce (IV)-Based CAU-24 with 1,2,4,5-Tetrakis (4-Carboxyphenyl) Benzene. *Dalton Trans.* **2016**, *45*, 18822–18826. [CrossRef] [PubMed]
92. Wu, G.; Yang, Y.-W. Macrocycle-Based Fluorochromic Systems. *Cell Rep. Phys. Sci.* **2024**, *5*, 101873. [CrossRef]
93. Cui, R. A Tb-MOF Anion, Porous Coordination Framework Constructed with Oxalate Ligand: Crystal Structure, Adsorption Properties, and Luminescence Sensing. *Dyes Pigm.* **2021**, *195*, 109669. [CrossRef]